

# Advances in Brain Tumor Therapy Based on the Magnetic Nanoparticles

Songbai Xu<sup>1</sup>, Guangxin Zhang<sup>2</sup>, Jiaomei Zhang<sup>1</sup>, Wei Liu<sup>2</sup>, Yicun Wang<sup>2</sup>, Xiyi Fu<sup>2</sup>

<sup>1</sup>Department of Neurosurgery, Department of Obstetrics, Obstetrics and Gynaecology Center, the First Hospital Jilin University, Changchun, People's Republic of China; <sup>2</sup>Department of Endocrinology, Jilin Provincial Key Laboratory on Molecular and Chemical Genetics, Department of Thoracic Surgery, the Second Hospital of Jilin University, Changchun, People's Republic of China

Correspondence: Yicun Wang; Xiyi Fu, Email wangyicun@jlu.edu.cn; fuxiyi@jlu.edu.cn

**Abstract:** Brain tumors, including primary gliomas and brain metastases, are one of the deadliest tumors because effective macromolecular antitumor drugs cannot easily penetrate the blood-brain barrier (BBB) and blood-brain tumor barrier (BTB). Magnetic nanoparticles (MNPs) are considered the most suitable nanocarriers for the delivery of brain tumor drugs because of their unique properties compared to other nanoparticles. Numerous preclinical and clinical studies have demonstrated the potential of these nanoparticles in magnetic targeting, nuclear magnetic resonance, magnetic thermal therapy, and ultrasonic hyperthermia. To further develop and optimize MNPs for the diagnosis and treatment of brain tumors, we attempt to outline recent advances in the use of MNPs to deliver drugs, with a particular focus on their efficacy in the delivery of anti-brain tumor drugs based on magnetic targeting and low-intensity focused ultrasound, magnetic resonance imaging for surgical real-time guidance, and magnetothermal and ultrasonic hyperthermia therapy. Furthermore, we summarize recent findings on the clinical application of MNPs and the research limitations that need to be addressed in clinical translation.

**Keywords:** magnetic nanoparticles, blood-brain tumor barrier, tumor therapy, drug delivery, brain tumor

## Introduction

Brain tumors are malignant tumors associated with high mortality rates and accounted for 1% of all new cancer cases worldwide in 2021. Additionally, brain tumors are the most prevalent solid tumors in adolescents and children and the leading cause of cancer-related death in men <40 years of age and women <20 years of age.<sup>1</sup>

Despite advancements in cancer treatment, the survival rates for brain tumors have seen minimal improvement in recent years, a contrast to the significant progress observed in the treatment of various other tumors. This can be attributed to three primary reasons. First, the early symptoms of brain cancer are not obvious, leading to late detection and subsequently missed opportunities for optimal treatment. Second, brain tumors are difficult to completely eliminate by surgery due to the infiltration of brain metastases into neural tissue. This challenge poses a significant threat to the central nervous system (CNS). Additionally, this challenge explains the poor prognosis and high recurrence rates associated with brain tumors. Third, immunotherapy is widely used for treating tumors (eg, hepatic carcinoma,<sup>2,3</sup> bladder cancer,<sup>4</sup> melanoma cancer,<sup>5</sup> lung cancer,<sup>6,7</sup> and breast cancer<sup>8</sup>) because antibodies can enter the tumor microenvironment and cellular. However, the blood-brain barrier (BBB) limits the clinical application of immunotherapy in brain tumors.

The BBB, a dense interface composed of microvascular endothelial cells, astrocyte endfeet, and pericytes,<sup>9</sup> regulates the exchange of substances between the CNS and the bloodstream.<sup>10,11</sup> The following features differentiate the BBB from other vascular endothelia: (1) The BBB is characterized by the presence of dense junctions between adjacent endothelial cells, effectively blocking the transport of water-soluble molecules but allowing the transport of lipid-soluble molecules and small molecules;<sup>12</sup> (2) Unlike other endothelia, the BBB lacks active transport and endocytosis mechanisms for regulating essential motifs and preventing the transfer of endogenous and exogenous toxic substances;<sup>10</sup> and (3) the absence of fenestration.<sup>13</sup> Several studies have indicated that brain tumor progression leads to the transformation of

the BBB into the blood-brain tumor barrier (BTB). Compared to the BBB of healthy individuals, the BTB is more permeable owing to the destruction of the basement membrane. Furthermore, the connections between the vascular endothelial cells are not dense, leading to the formation of pores with a diameter of 10–30 nm.<sup>9</sup> This pore size indicates that nanoparticles hold great promise in the treatment of therapy of brain tumors.

Nanoparticles, owing to their general properties, such as small size (1–100 nm), enhanced permeability and retention effect (EPR), and high permeability in tumors, have emerged as valuable tools in tumor therapy. In addition to the general characteristics of nanoparticles, some magnetic nanoparticles (MNPs) have unique properties, including high permeability, stable surface properties, high saturation magnetization (MSat), magnetocaloric effect, and high-intensity focused ultrasound. These unique properties of MNPs make them valuable tools for tumor imaging, highly effective delivery of molecules<sup>14,15</sup> (such as genes,<sup>16,17</sup> proteins, and other drugs<sup>18</sup>), targeted immunotherapy,<sup>19</sup> targeted chemotherapy,<sup>20</sup> magnetothermal therapy,<sup>21–23</sup> and focused ultrasound therapy.<sup>24,25</sup>

Because MNPs have received considerable attention in nanomedicine research and clinical therapy, this review focuses on the production, classification, and application of MNPs. This review sheds light on current advances in the clinical application of MNPs in the treatment of brain tumors (Figure 1).

### MNPs

MNPs are a class of nanoparticles that have found extensive application in various biomedical areas, including diagnosis, imaging, and therapy, due to their unique and distinguished magnetism when subjected to a magnetic field. This magnetism plays a “double-edged role” in nanomedicine applications of MNPs. Notably, the magnetism of MNPs

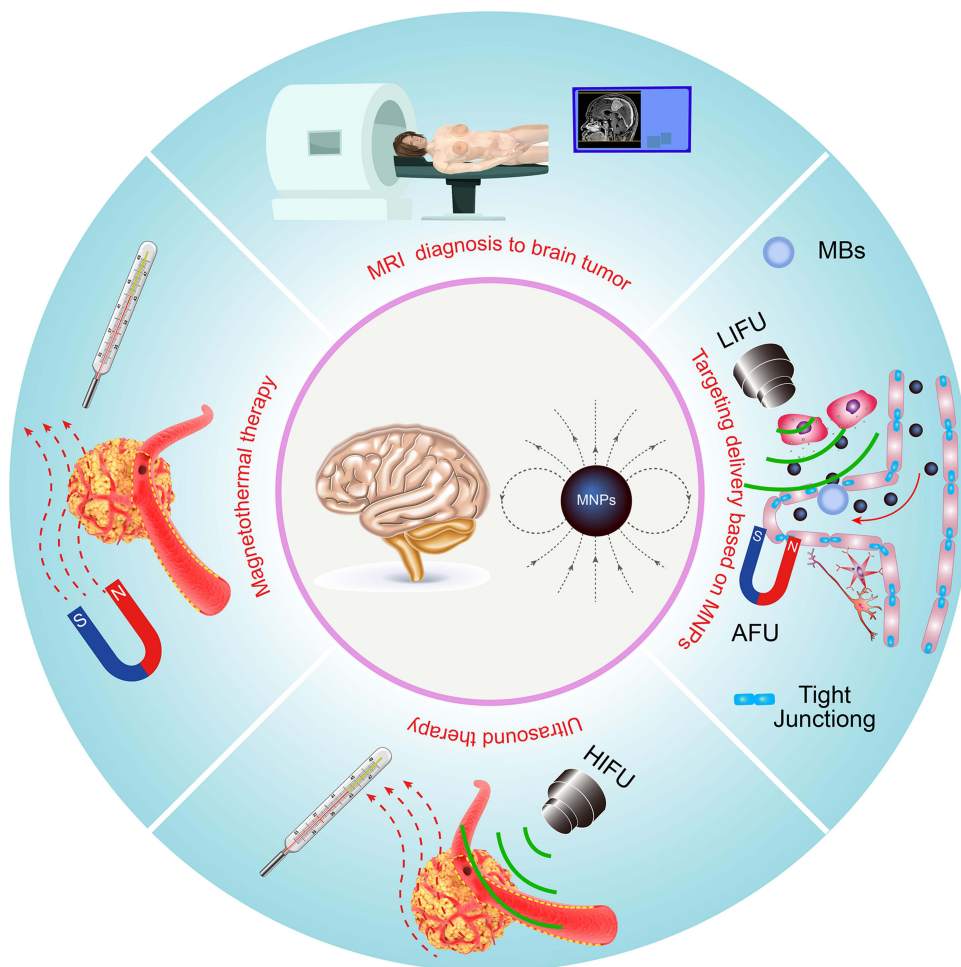


Figure 1 Overview of magnetic nanoparticles (MNPs) for brain tumor therapy.

enables them to provide signals in magnetic resonance imaging (MRI), enhance the detection of low-concentration molecules, and provide heat and iron elements in therapy. The ability of MNPs to maintain stable dispersion in solution without aggregation or precipitation, coupled with their responsiveness to external magnetic fields through Néelian and Brownian relaxations, further enhances their versatility.<sup>26,27</sup> However, excessively strong magnetism can cause MNPs to attract each other and aggregate, inducing embolism in blood capillary vessels. Therefore, the modification of MNPs to regulate magnetism intensity is vital in the medical application of MNPs.

## Classification of MNPs

MNPs commonly comprise two parts: a core magnetic component (such as iron, nickel, or cobalt) and a functional part. Therefore, the MNPs could be classified into different types based on the elements and functional components.

### Monocomponent MNPs

#### Fe, Ni, and Co-Based MNPs

Iron nanoparticles (Fe NPs) are the most extensively used MNPs due to their unique physical and chemical properties that allow them to permeate biological membranes and reach diverse tissues and cells. Notably, Fe NPs induce the production of reactive oxygen species (ROS), including hydrogen peroxide ( $\text{H}_2\text{O}_2$ ), hydroxyl radical ( $\bullet\text{OH}$ ), and superoxide anion ( $\text{O}^{2-}$ ).<sup>28</sup> Additionally, the different degrees of pyrophoricity and reactivity of FeNPs may induce unwanted reactions.<sup>29</sup>

In 2003, monodisperse nickel nanoparticles (Ni NPs) were formulated by reducing Ni (acac)<sub>3</sub> in hexadecylamine (HDA).<sup>30</sup> Monodisperse Ni NPs have been used in various materials, including magnetic materials,<sup>31</sup> sensor materials,<sup>32</sup> medical motifs,<sup>33</sup> optics,<sup>34,35</sup> and catalysts.<sup>36–38</sup> However, the application of NiNPs in cancer treatment has not been reported.

Cobalt NPs (Co NPs), with sizes ranging from 2 to 11 nm, have been successfully formulated using different methods.<sup>39,40</sup> Unlike FeNPs, which are characterized as soft magnets due to a rapid increase in magnetization when exposed to an external magnetic field (EMF) and a subsequent decrease or elimination of magnetization upon EMF withdrawal, Co NPs exhibit the properties of hard magnets by retaining residual magnetization. This unique property of Co NPs has attracted the interest of researchers.<sup>41</sup> In the presence of unsaturated hemoglobin, Co NPs do not induce misleading signals, whereas Fe NPs do.<sup>42</sup> Some other unique properties of Co NPs (ie, high mechanical hardness, high Curie temperature, and large magnetic multiaxial anisotropy) may make them potentially useful in diagnostic and therapeutic applications (eg, gene therapy and drug release). Unfortunately, the progress of medical applications of Co NPs has been limited, possibly due to the associated higher instability and toxicity compared to Fe NPs.<sup>43</sup> Therefore, it is necessary to study methods to reduce toxicity through surface modification and regulation to align with clinical standards.<sup>44</sup>

#### Metal Alloy MNPs

Some metal alloy nanoparticles, such as iron–palladium (FePd)<sup>45</sup> and iron–platinum (FePt),<sup>46,47</sup> are promising MNPs. These alloys exhibit superparamagnetism, high magnetic crystallinity, and chemical stability. Several studies have reported that the heating response of CoFe alloy nanoparticles to a variable magnetic field could be determined by regulating the proportion of cobalt.<sup>48,49</sup> Compared to magnetite ( $\text{Fe}_3\text{O}_4$ ) and cobalt ferrite ( $\text{CoFe}_2\text{O}_4$ ) MNPs, CoFe NPs with an adjustable thermal response exhibit high-efficiency therapeutic potential and specific loss power (SLP) in tumors.<sup>49,50</sup>

#### Metal Carbide MNPs

Although metal (Fe, Co, and Ni) carbide MNPs have piqued the interest of researchers due to their exceptional magnetic characteristics and stability,<sup>51</sup> their application has barely advanced as their synthesis requires harsh conditions and there are challenges in controlling their size and morphology.<sup>52</sup>

#### Metal Oxide MNPs

Metal oxide MNPs are the most widely used MNPs in the biomedical field.<sup>53</sup> Notably, iron oxide MNPs are currently the only FDA-authorized MNPs for use in humans.<sup>54</sup> Iron oxide can exist in four stable chemical compositions, namely magnetite ( $\text{Fe}_3\text{O}_4$ ), wüstite (FeO), hematite ( $\alpha\text{-Fe}_2\text{O}_3$ ), and maghemite ( $\gamma\text{-Fe}_2\text{O}_3$ ). A growing body of preclinical and clinical studies have indicated that iron oxide MNPs can interact with immune system cells to stimulate their immune

recognition of tumors.<sup>55–57</sup> Despite the extensive use of iron oxide MNPs in immunotherapy, the underlying mechanisms are not fully understood. In a study by Daldrup-Link et al, ferumoxytol injection into tumor-bearing mice significantly delayed tumor growth. Furthermore, an injection of iron oxide MNPs into T cell-deficient mice before cancer cell injection prevented tumor formation. This preventive effect was attributed to the nanoparticles inducing the polarization of macrophages into the M1 phenotype rather than stimulating T cells.<sup>57</sup> However, other studies have shown that iron oxide MNPs induce T cell-mediated immune effects that kill cancer cells.<sup>55,56,58,59</sup>

## Multicomponent MNPs

### Heterostructure MNPs

Heterostructure MNPs are composed of a magnetic component and other components and garner immense interest because they possess magnetic and other unique properties (eg, optical properties, catalytic activity, and biocompatibility).<sup>60</sup>

(1) The most common structures of heterostructured MNPs are the MNP core and a shell structure wrapped around the exterior. Several core-shell-structured MNPs have been produced over the last few decades, including  $\text{Fe}_3\text{O}_4@\text{ZnO}$ ,<sup>61</sup>  $\text{Fe}_3\text{O}_4@\text{TiO}_2$ ,<sup>62</sup>  $\text{Fe}_3\text{O}_4@\text{Au}$ ,<sup>63</sup>  $\text{Fe}_3\text{O}_4@\text{poly (dopamine)}$ ,<sup>64</sup>  $\text{Fe}_3\text{O}_4@\text{C}$ ,<sup>65</sup>  $\text{CaSO}_4@\text{Fe}_2\text{O}_3@\text{SiO}_2$ ,<sup>66</sup>  $\text{Fe}_3\text{O}_4@\text{PEG-Ag}$ ,<sup>67</sup>  $\text{FePt}@\text{Fe}_2\text{O}_3$ ,<sup>68</sup>  $\text{Fe}_3\text{O}_4@\text{humic acid}$ ,<sup>69</sup>  $\text{Fe}_3\text{O}_4@\text{MnO}$ ,<sup>70</sup>  $\text{Fe}_3\text{O}_4@\text{chitosan}$ ,<sup>71</sup> and  $\text{CoFe}_2\text{O}_4@\text{MnFe}_2\text{O}_4$ .<sup>72</sup> Among these, magnetic mesoporous silica nanocomposites (M-MSNs), which comprise a  $\text{Fe}_3\text{O}_4$  core wrapped in a mesoporous silicon shell, are widely used in the biomedical field because of their superior dispersibility and graft modification potential compared to bare  $\text{Fe}_3\text{O}_4$  nanoparticles.<sup>73</sup>

(2) Some irregularly shaped heterostructured MNPs have also been synthesized in recent years. Notably, Gao et al<sup>74</sup> prepared FeP-Au heterostructure MNPs. Additionally, Hou et al<sup>75</sup> demonstrated that the morphology of FePt-Au hybrid nanoparticles could be controlled by adjusting the size of FePt and the type of atmosphere.

### Magnetic Metal-Organic Framework (MOF)

Magnetic MOFs are another type of heterostructure MNPs that have gradually gained prominence in mainstream research.<sup>76</sup> Despite their high absorption capacity, the absorption bandwidth of typical metal and alloy MNPs is considerably low for clinical applications. The carbon-based part of the magnetic MOF can address this issue.<sup>77</sup> Magnetic MOF nanoparticles with Fe,<sup>78</sup> Co,<sup>79</sup> Ni,<sup>80</sup> Fe-Co,<sup>77</sup> Fe-Ni,<sup>81</sup> Co-Ni,<sup>82</sup> and Fe-Co-Ni<sup>83</sup> have been successfully synthesized. In 2021, Khoobi et al used the  $\text{Fe}_3\text{O}_4@\text{ALA-Zn}$  magnetic MOF to conduct an MRI of a brain tumor and kill cancer cells.<sup>84</sup> In the same year, Tian et al<sup>85</sup> synthesized a magnetic MOF nanoprobe ( $\text{CH}_4\text{T}@\text{MOF-PEG-AE}$ ) and injected the nanoparticle into glioblastoma-bearing mice. The nanoprobe, used in conjunction with MRI and near-infrared (NIR)-II fluorescence imaging with spatiotemporal resolution, facilitated the surgical removal of malignancies. Moreover, photothermal therapy of the magnetic MOF nanoprobe yielded surprisingly satisfactory results.

## Synthesis of MNPs

Over the past few decades, MNPs have been applied in several specialized fields, including biomedicine, biotechnology, catalysis, and the development of magnetic chemistry thermoelectric materials. The synthetic method for MNPs is crucial since it might impact their physicochemical characteristics, stability, mobility, and effectiveness in pollution removal.<sup>86</sup> Generally, the synthesis of MNPs involves either a bottom-up (atoms and molecules are combined to prepare NPs of different sizes) or a top-down approach (synthesis begins with bulk material that is depleted to produce NPs). The synthetic methods encompass chemical synthesis, physical synthesis, and biological synthesis.

### Chemical Synthesis

Chemical synthesis approaches for MNPs primarily involve bottom-up approaches, such as hydrothermal synthesis, sol-gel formation, thermal decomposition, and coprecipitation.

(1) Hydrothermal synthesis, also known as solvothermal synthesis, is an effective solution reaction-based method for producing MNPs at high temperatures and pressures.<sup>86</sup> This method enables the production of uniform-sized MNPs by controlling the degree of mineral solubility in water, thus influencing crystal formation.<sup>87</sup> The hydrothermal approach is

preferred over the sol-gel method and other methods due to its ability to produce nanoparticles of the desired form, size, high crystallinity, and stable composition. Despite these advantages, the hydrothermal synthesis process requires specialized equipment and caution due to the necessary high pressure and temperature conditions. The MNPs produced via this method are very effective in strengthening or weakening the superparamagnetic property. Several researchers have attempted to synthesize smaller MNPs. In 2023, Abdollahi's group revealed that MNPs with hydrodynamic diameters of 28.74 and 24.88 nm could be synthesized at pH=11 and 12, respectively.<sup>88</sup>

(2) The sol-gel method is another heating synthesis technique. With this technique, metal salts are initially dissolved in solvents, with continuous stirring, to obtain a uniformly dispersed sol, followed by continuous heating to improve the interaction between particles (such as van der Waals forces). Ultimately, a gel forms as the solvent completely evaporates.<sup>89</sup> The sol-gel process requires no specific equipment and can be conducted at ambient temperature, making it a less expensive technology. Additionally, this method allows for straightforward control of the composition, shape, and size of MNPs. MNPs produced by this process have high purity, good crystallinity, and adjustability. However, under specific circumstances, by-products may be produced, necessitating further purification to obtain pure MNPs. Additionally, the sol-gel process is associated with longer reaction times, and the presence of chemical solvents can introduce toxicity concerns.

(3) The thermal decomposition approach is used to synthesize MNPs under high temperatures using organometallic precursors. This technique results in the production of MNPs with great crystallinity, well-determined shape, and regulated size. Adjustments are made to the type of surfactant and solvent, reaction time, aging duration, and temperature based on the desired form and size. This process is regarded as one of the most effective techniques for producing large amounts of MNPs of the same form and size.<sup>90</sup> In 2023, Insausti et al introduced an improved thermal decomposition method to synthesize MNPs based on the thermolysis of bimetallic oleates ( $\text{Fe}_{3-n}\text{MnOl}_{9-n}$ ).<sup>91</sup> They demonstrated that the synthesized MNPs exhibited highly homogenous sizes as small as 16 nm and possessed large saturation magnetization values ( $\geq 86 \text{ Am}^2/\text{kg}$  at room temperature). Remarkably, the MNPs showed a significant magnetothermal efficiency ( $> 600 \text{ W/g}$ ) while remaining within clinical safety limits (36 kA/m and 125 kHz), suggesting that the improved thermal decomposition method could be employed to synthesize MNPs suitable for clinical application.

(4) The coprecipitation approach is the most common method for synthesizing MNPs, offering convenience in controlling both the size and surface properties of MNPs. Notably, the coprecipitation method also ensures the production of large quantities of MNPs for clinical use. However, a drawback of the coprecipitation process is the challenge of controlling the form of the MNPs.<sup>92</sup> Several MNPs, including  $\text{MgFe}_2\text{SO}_4$ ,<sup>93</sup>  $\text{MnFe}_2\text{O}_4$ ,<sup>94</sup>  $\text{Fe}_3\text{O}_4$ ,<sup>95,96</sup>  $(\text{Zn}_x\text{Mn}_{1-x}\text{Fe}_{0.6})\text{Fe}_2\text{O}_4$ ,<sup>97</sup>  $\text{Co}_{1-x}\text{Cu}_x\text{Fe}_2\text{O}_4$ ,<sup>98</sup>  $\text{ZnFe}_2\text{O}_4$ ,<sup>99</sup> and copper ferrite<sup>100</sup> have been synthesized using the coprecipitation approach.

## Physical Synthesis

Physical synthesis methods for MNPs typically follow the “top-down” approach. These methods involve techniques such as laser evaporation, mechanical milling, and wire explosion. Laser evaporation is a straightforward method that produces nanoparticles via condensation from a gaseous or liquid phase.<sup>101</sup> This method is inexpensive, has a high production rate, and is eco-friendly. Mechanical milling is a simple and convenient process that produces various particles through mechanical grinding. Ball milling, the most common mechanical milling method, is convenient, inexpensive, highly efficient, and environmentally friendly.<sup>102</sup> However, the major limitation of ball milling is that the purity of the product is insufficient.<sup>89</sup> Wire explosion, which causes the evaporation of a metal wire under a strong electric current, is a promising physiochemical approach.<sup>103</sup> This method also has some disadvantages, such as product contamination, high requirements for energy, and the production of non-monodispersed MNPs.<sup>104–106</sup>

## Biological Synthesis

The biological synthesis of MNPs has garnered considerable interest owing to its eco-friendly, efficient, and clean process. MNPs synthesized via this method are comparatively biocompatible but lack ideal dispersibility.<sup>107</sup> The biosynthesis of MNPs involves microorganisms, plant extracts, and animals.<sup>108</sup> Microbial synthesis occurs primarily through the adsorption of metal ions and reduction mineralization.<sup>109</sup> The plant extract synthesis approach depends on water-soluble metabolites such as polyphenols, alkaloids, and citric acid.<sup>110,111</sup> Magnetite, widely distributed in living

organisms, helps sense the earth's magnetic field to determine direction.<sup>112</sup> Biologically synthesized MNPs can be used as catalysts in photocatalysis and Suzuki-Miyaura reactions. However, this method has some drawbacks, including poor dispersibility and low yield of MNPs, which need to be worked upon.

In 2023, Anwer used microalgae *Spirulina* sp. as a replacement for anise fruit extract in the biosynthesis of MNPs.<sup>113</sup> The general procedure involved mixing ferrous chloride ( $\text{FeCl}_2 \cdot 4\text{H}_2\text{O}$ ) and ferric chloride ( $\text{FeCl}_3 \cdot 6\text{H}_2\text{O}$ ) at a 2:1 molar ratio, followed by heating at 70°C under a nitrogen atmosphere for 10 min. Subsequently, microalgae *Spirulina* sp. was added to the mixture for 20 min until the yellow color turned black. Finally, NaOH solution was added to the mixture at a flow rate of 2 mL/min to allow magnetite precipitation. The scanning electron microscopy (SEM) results indicated that the diameter of the MNPs ranged from 52.05 to 55.98 nm. In the same year, Othman et al also employed anise fruit extract for the biosynthesis of MNPs.<sup>114</sup> Their procedure generally involved mixing ferrous sulfate ( $\text{FeSO}_4 \cdot 7\text{H}_2\text{O}$ ) and ferric chloride ( $\text{FeCl}_3$ ) at a 1:2 molar ratio, followed by heating at 80°C under a nitrogen atmosphere for 10 min. Subsequently, the mixture was combined with the anise fruit extract for 5 min, and a 5% NaOH solution was slowly added to the mixture to uniformly produce magnetite precipitation. The transmission electron microscopy (TEM) results indicated this method could synthesize smaller MNPs with diameters between 18 and 33 nm.

## Biomedical Application of MNPs

Based on their different mechanisms of action, MNPs can be used in three categories of tumor therapy. First, MNPs can be used as nanoscale magnets to enhance the delivery of drugs into tumors with high efficiency. This is achieved by leveraging the magnetic force experienced by MNPs, allowing them to move against the field gradient.<sup>115</sup> Recent research suggests that MNPs could be used as molecular force transducers to activate specific receptors on cancer cells, and subsequently induce their apoptosis.<sup>43,116–118</sup> Second, the MNPs could be employed as T1 or T2 contrast agents in MRI. MNPs have been used, in conjunction with MRI, to track tumors for over 30 years.<sup>119,120</sup> Third, MNPs have been used since 1957 to transform electromagnetic energy into heat energy, a phenomenon known as thermal treatment.<sup>121</sup>

## Targeted Delivery Based on MNPs

### Targeted Delivery Under EMF Guidance

Targeted delivery under EMF guidance is a strategy that exploits the unique properties of nanoparticles, particularly MNPs, to enhance the delivery of drugs into tumors via relatively inefficient passive targeting based on enhanced permeability and retention (EPR).<sup>122</sup> The EPR mechanism involves the permeation of nanoparticles into tumor capillaries, reduction of blood flow by dilated curved capillaries, and the subsequent retention of the nanoparticles in the tumor.<sup>123</sup> Meanwhile, the 200–2000 nm pores in tumor blood vessels are sufficient to allow nanoparticles to pass into the tumor microenvironment.<sup>124</sup> Common MNPs, which have a small size (3–200 nm in diameter), can accumulate in brain tumors via the EPR mechanism. To optimize the targeting effects, MNPs are often coated with weaker negative charges, such as those found on cell membranes, polyethylene glycol (PEG), and polyethyleneimine (PEI). This coating helps stabilize MNPs in the blood, as strongly negatively charged particles are more easily eliminated by the reticuloendothelial system (RES). Active targeting strategies have attracted increasing attention as a method for improving targeting effects because they are more efficient than EPR-based passive targeting. In active targeting, MNPs are conjugated with ligands that can recognize highly expressed receptors on the membranes of cancer cells and tumor-associated cells. For instance, many ligands such as transferrin,<sup>125–130</sup> folate,<sup>131–133</sup> hyaluronic acid,<sup>134,135</sup> aptamers,<sup>136,137</sup> antibodies,<sup>15,138–140</sup> and peptides<sup>141–144</sup> have been conjugated with MNPs for active targeted delivery into brain tumor sites.<sup>145</sup>

MNPs present unique advantages for drug delivery into brain tumors, particularly due to their strong response to EMF. Generally, by placing an EMF at the brain tumor site, drug-carrying MNPs can navigate the circulatory system and accumulate locally in the tumor by magnetic force. This strategy is called magnetic targeting (MT). Several studies have demonstrated that MT can achieve higher efficiency compared to EPR-mediated passive targeting and ligand-receptor interaction-mediated active targeting.<sup>146–149</sup> However, EMF is limited in treating superficial tumors due to its short active reach-out range.<sup>150</sup> To overcome this shortcoming, a gradient magnetic field was developed and exhibited satisfactory MT.<sup>151</sup>

In 2023, Chen et al<sup>152</sup> synthesized citric-acid-coated MNPs (CMNPs) and encapsulated them in thin films to prepare thermosensitive cationic magnetic liposomes (TCMLs). These TCMLs were then loaded with CPT-11 (irinotecan) to prepare TCML@CPT11/shRNA. Glioblastoma (U87)-bearing nude mice were subsequently injected with the TCML@CPT11/shRNA, and MT was performed using an alternating magnetic field (AMF). Notably, TCML@CPT11/shRNA+AMF treatment exhibited a significantly better therapeutic effect compared to TCML@CPT11/shRNA treatment (Figure 2).

## Targeted Delivery via Focused Ultrasound

The permeability of the BTB is higher than that of the BBB, but it remains heterogeneous and occasionally behaves similarly to a healthy BBB.<sup>9</sup> The development of a novel controllable approach to improve the permeability of the BTB has garnered research interest. Magnetic resonance-guided focused ultrasound (MRgFUS) is a novel physical approach to transiently modulate the structure between the tumor microenvironment and neurovascular unit and deliver drugs into brain tumors.<sup>153</sup> MRgFUS can be categorized as low-intensity focused ultrasound (LIFU) and high-intensity focused ultrasound (HIFU). LIFU is commonly used to deliver nanomedicines into brain tumors by producing microbubbles

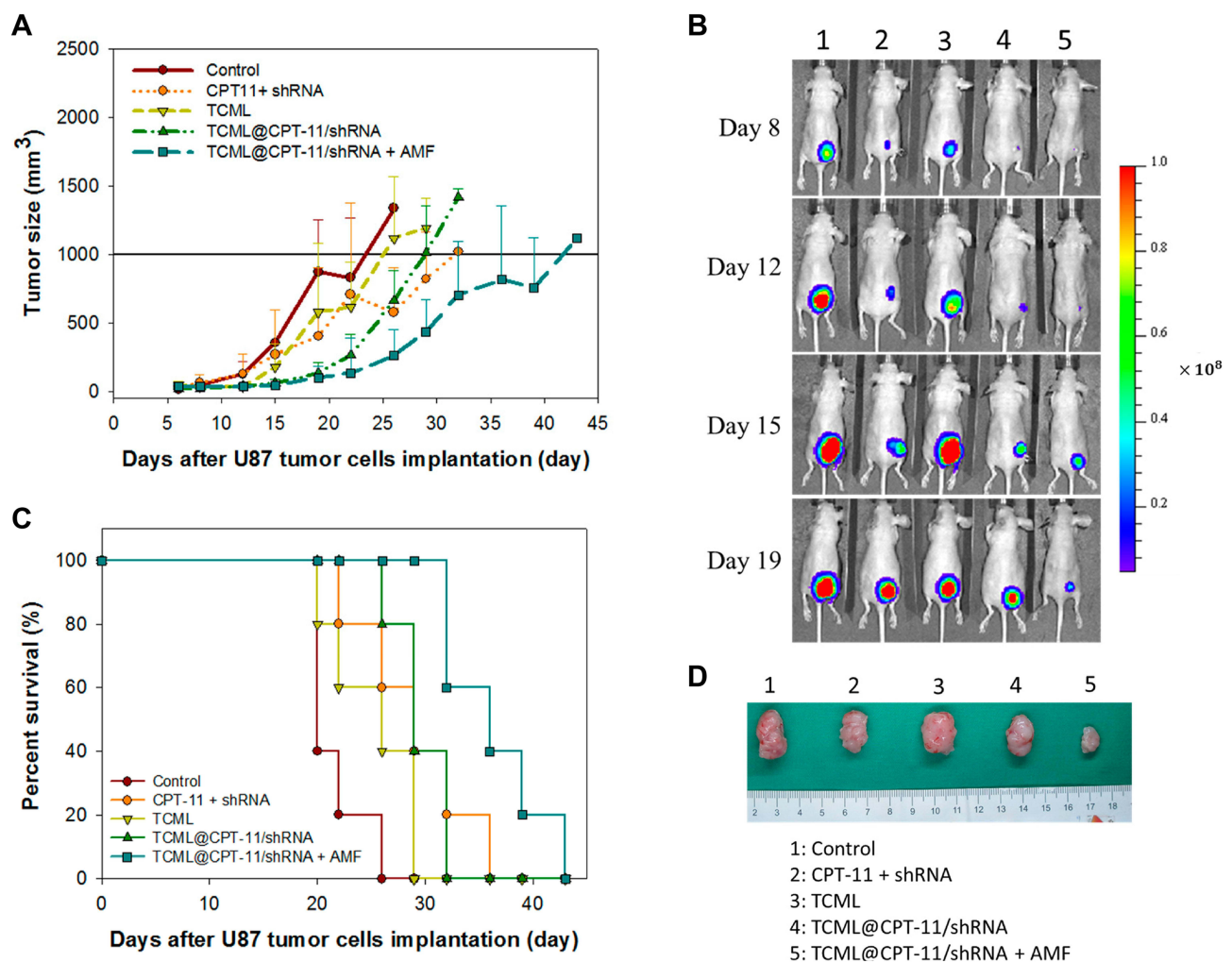


**Figure 2** Therapy with TCML@CPT11/shRNA nanoparticles for glioblastoma (U87) tumors.

**Notes:** (A) Changes in tumor size after treatment with MNPs. (B) Bioluminescence imaging (BLI) of tumor-bearing mice treated with TCML@CPT11/shRNA+AMF. (C) Survival curves after therapy. (D) Images of tumors treated for 22 days. Adapted from Lu Y-J, Hsu H-L, Lan Y-H, Chen J-P. Thermosensitive Cationic Magnetic Liposomes for Thermo-responsive Delivery of CPT-11 and SLP2 shRNA in Glioblastoma Treatment. *Pharmaceutics*. 2023;15(4):1169.<sup>152</sup>

(MBs). In contrast, HIFU can be used for the mechanical destruction and thermoablation of tumors by inducing the movement of magnetic nanoparticles and magnetoheat.<sup>154</sup>

When stimulated by LIFU, MBs expand or contract, opening the tight junctions of the BBB/BBB and delivering drugs into brain tumors.<sup>153,155</sup> Several studies have reported that some drugs (eg, trastuzumab,<sup>156</sup> bevacizumab,<sup>157</sup> carboplatin,<sup>158,159</sup> temozolomide,<sup>160</sup> methotrexate,<sup>161</sup> and doxorubicin<sup>162</sup>) can be delivered through the BTB using LIFU. Notably, LIFU has been demonstrated to have no significant side effects, and the pores or “windows” it forms on the BBB close within 6–8 h, preventing prolonged exposure and potential damage to neurons.<sup>163</sup>

In 2010, Liu et al<sup>25</sup> synthesized MNPs with a diameter of 12.5 nm. They conjugated epirubicin with these MNPs to prepare epirubicin-MNP. Rats bearing C6 tumors were injected with epirubicin-MNPs, and 10 days later, they were subjected to LIFU. TEM revealed the appearance of interendothelial clefts in rats treated with LIFU. Notably, the survival period after treatment with the combination of epirubicin-MNPs and LIFU/MT was extended by 30.5 days.

Although MNPs can accumulate at the tumor site under the guidance of magnetic field/focused ultrasound, they cannot do so without entrance into the normal brain tissues (such as neurons and glial cells). This occurrence is because the surface of the MNPs lacks ligands that recognize receptors on the surface of tumor cells. Unfortunately, there has been little research on the coupling of tumor-specific ligands to the surface of MNPs to combine MT/ focused ultrasound targeting and molecular active targeting to achieve anti-brain tumor drug delivery. We believe that the next step in targeted delivery into brain tumors using MNPs will be to seek breakthroughs in this direction.

## MRI Using MNPs

MRI is the major soft tissue diagnostic technique used in clinical settings due to several unique advantages, including enhanced soft tissue contrast, high resolution, and excellent anatomic detail.<sup>164</sup> Meanwhile, MRI does not exhibit the potential radioactive hazards commonly associated with computed tomography (CT) or positron emission tomography (PET).<sup>165</sup> While MRI provides valuable information, the inherent signals in MRI, determined by tissue characteristics such as relaxation time and proton density, often lack sufficient contrast for precise imaging. Therefore, a contrast agent needs to be injected into the body before testing. The exogenous contrast agents used in MRI are categorized as T1 (positive) and T2 (negative) contrast agents.

T2 contrast agents are frequently mistaken for several endogenous components, including blood clots, hemorrhage, air, and calcification. Hence, T1 contrast agents are typically preferred in clinical settings.<sup>166</sup> Unfortunately, the T1 contrast agents currently in use (eg,  $Gd^{3+}$ - and  $Mn^{2+}$ -based agents) occasionally exhibit toxicity. Iron oxide MNPs are alternative T1 contrast agents due to their marked biocompatibility; however, because of their lower  $r_1$  value, which is much lower than the  $r_2$  value of calcium, most of them are now used as T2 contrast agents. Notably, researchers are attempting to regulate the  $r_2/r_1$  ratio by adjusting the particle surface state and size to improve their suitability as T1 contrast agents.

When the diameter of iron oxide MNPs is smaller than 1.8 nm, most of their spins become canted, conferring virtually paramagnetic characteristics to these nanoparticles. Some studies have demonstrated that these MNPs could be employed as T1 contrast agents, given their  $r_1$  relaxivity and  $r_2/r_1$  ratio of up to  $4.78 \text{ mM}^{-1}\text{s}^{-1}$  and 3.67, respectively.<sup>167,168</sup> However, the thickness of the organic motif coated on MNPs always affects their use as T1 contrast agents.<sup>169</sup> Research indicates that adjusting the thickness can reduce the aggregation of these MNPs and decrease the T2 contrast.<sup>170</sup>

MRI proves valuable in diagnosing tumors due to the distinct pathological structures of tumor vessels. These structures include excessive branching, greater diameters, endothelial fenestrae, leaky holes, and a discontinuous basement membrane.<sup>122,171,172</sup> These unique structures facilitate the accumulation of MNPs in the tumor microenvironment via the EPR effect (passive targeting). Active targeting strategies have been developed in recent years to increase the accumulation of MNPs in tumors for highly sensitive and accurate MRI.<sup>173</sup> Various tumor biomarkers, including ligands present on the cancer cell membrane and molecules in the tumor microenvironment, have been reported. These biomarkers include engineered exosomes,<sup>15</sup> heptamethine cyanine,<sup>174</sup> antibodies,<sup>175,176</sup> growth factors,<sup>177</sup> polymers,<sup>178</sup> ligand protein,<sup>179–181</sup> peptides,<sup>182</sup> and aptamers,<sup>183</sup> which have been conjugated with MNPs to improve MRI efficiency.

In 2021, Wang<sup>184</sup> et al conjugated Cy5.5 fluorescence dye with  $Fe_3O_4$  with a 190 nm diameter to prepare a  $Fe_3O_4$ -Cy5.5 nanoprobe. The  $Fe_3O_4$ -Cy5.5 nanoprobe was loaded into macrophages to produce an  $MFe_3O_4$ -Cy5.5 magnetic



photothermal nanoprobe. After the  $\text{MFe}_3\text{O}_4\text{-Cy5.5}$  magnetic photothermal nanoprobe was injected into glioblastoma-bearing mice, hypointense shadows appeared around the tumor and maintained high contrast for 5 days. The MRI signal based on  $\text{MFe}_3\text{O}_4$  matched the fluorescence imaging based on Cy5.5. Surprisingly, the authors found that MNPs could also yield photoacoustic images for cross-validation with MRI (Figure 3A-C). One year later, another group of researchers<sup>185</sup> prepared sub-5 nm ultrafine IONP (uIONP) and coated them with oligosaccharides. After 20 min of intravenous injection into glioblastoma-bearing mice, sub-5 nm oligosaccharide-coated uIONP accumulated in the tumor. The MRI results revealed that after 40–60 min of injection, the signal from the T1-enhanced MRI contrast gradually peaked in the tumor but not in normal tissue (Figure 3D-F). The T1-enhanced MRI contrast of uIONP was similar to that of the clinical Gd contrast agent.

## Thermal Therapy Using MNPs

Thermal therapy has great potential in the treatment of multiple tumors, as it can directly kill cancer cells at high temperatures. The resulting exposure of tumor cell contents causes an immune response in patients. However, the traditional process of thermotherapy for tumors, especially photothermal therapy, can only be used to treat surface or superficial tumors because it is constrained by the depth of light penetration. Fortunately, magnetic fields and ultrasound can penetrate deep tissues (eg, skin, skull, and brain tissue) and stimulate MNPs in brain tumors to generate heat that facilitates tumor hyperthermia.

## Magnetothermal Therapy Using MNPs

### Thermal Ablation

Cells die upon exposure to temperatures above 50 °C.<sup>186,187</sup> Thermal ablation, which can cause tumor necrosis and carbonization, typically involves the insertion of electrodes and the transfer of heat into the tumor tissue. However, this approach has limitations, especially in the treatment of brain tumors due to the invasive nature of electrode insertion. The properties of MNPs and magnetic fields can help overcome this limitation. In the thermal ablation process using MNPs, the nanoparticles are injected into the bloodstream and accumulate at the tumor site. Upon accumulation, these MNPs generate heat when exposed to an EMF, leading to the destruction of surrounding cells. To generate sufficient heat, MNPs with SLP values are best suited for thermal ablation. Although the SLP directly affects treatment efficiency, there are safety concerns that the product of field amplitude ( $Hf$ ) and frequency must be less than  $5 \times 10^9$  A /m/s. A European company called MagForce Nanotechnologies AG has designed an AFM applicator (MFH 300FTM) that generates a variable magnetic field with a frequency of 100 kHz, 2–15 kA/m, suitable for the treatment of brain tumors.<sup>188</sup> A clinical study by Jordan et al in 2011 involved intracranial injection of MNPs into the tumors of 66 patients, followed by the application of an AMF to achieve a temperature of 50 °C. Notably, the overall survival was prolonged to 23.2 months after receiving the therapy<sup>189</sup> (Figure 4A–G). In 2022, Chen et al combined stereotactic laser ablation (SLA) and consolidation stereotactic radiosurgery (cSRS) to treat brain tumors metastasized from lung cancer, breast cancer, gastrointestinal cancer, melanoma cancer, ovarian cancer, urothelial cancer, and laryngeal cancer<sup>190</sup> in a study involving 20 patients. They injected 5–6 Gy MNPs and heated them to 43–60°C. The results indicated that 73% to 100% of the brain tumors were ablated, with 5 patients surviving for more than 12 months (Figure 4H–J).

To avoid killing adjacent normal cells at high temperatures, localized AMF is used to selectively heat precise tumor sites. In 2009, Atalar et al employed a perpendicular magnetic field of equal or greater amplitude than the common static field. Only MNPs in the magnetic field's free zone generated heat,<sup>191</sup> limiting the area heated due to magnetothermal therapy and eliminating side effects.

### Apoptotic Hyperthermia

Although magnetothermal therapy can help rapidly eliminate tumors, imprecisely controlled high temperatures can damage normal tissues surrounding tumors. Therefore, a novel magnetic thermal therapy that operates at a lower temperature compared to the thermal ablation method has garnered clinical attention. Recently, mild apoptotic hyperthermia therapy was reported. This method operates at a temperature window of 42–45°C<sup>192</sup> to induce cancer

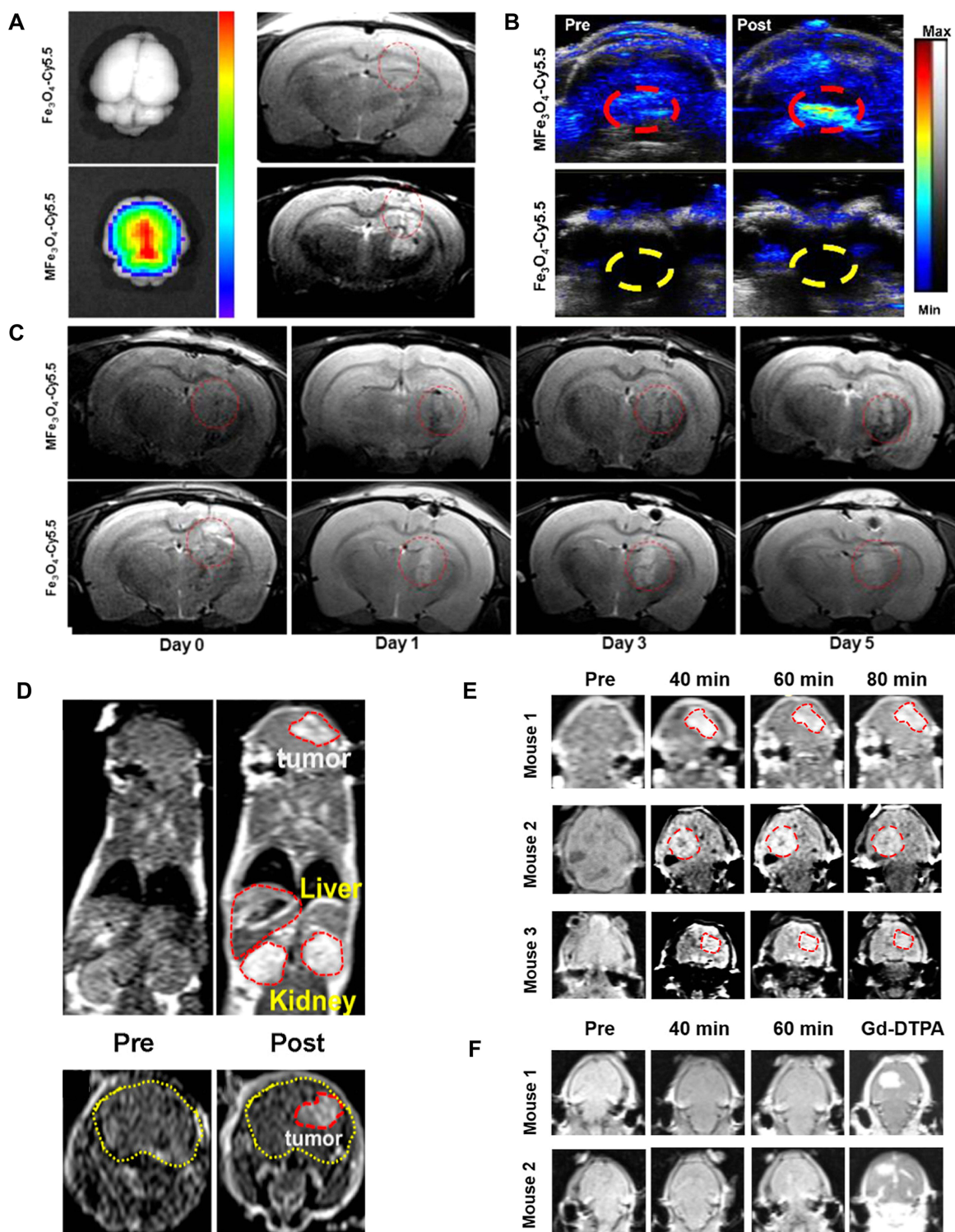


**Figure 3** (A) Optical imaging (left) and MRI (right) 24 h after the injection of Fe<sub>3</sub>O<sub>4</sub>-Cy5.5 and MFe<sub>3</sub>O<sub>4</sub>-Cy5.5 through the tail vein (B) Photoacoustic imaging of nanoparticles injected into tumor-bearing rats. (C) MRI of glioma-bearing rats injected with MFe<sub>3</sub>O<sub>4</sub>-Cy5.5 (top) and Fe<sub>3</sub>O<sub>4</sub>-Cy5.5 (bottom). (D) Coronal views (top) and axial views (bottom) of pre- and post-contrast-enhanced T1-weighted spin-echo MRI of intracranial brain tumors. (E and F) T1-weighted MRI of mice before and after the intravenous injection of IONP. (E) and 10 nm core size (F).

**Notes:** (A–C) Adapted with permission from Wang S, Shen H, Mao Q et al. Macrophage-Mediated Porous Magnetic Nanoparticles for Multimodal Imaging and Postoperative Photothermal Therapy of Gliomas. *ACS Appl Mater Interfaces*. 2021;13(48):56825–56837. Copyright 2021 American Chemical Society.<sup>184</sup> (D–F) Adapted with permission from Xie M, Li Y, Xu Y et al. Brain Tumor Imaging and Delivery of Sub-5 nm Magnetic Iron Oxide Nanoparticles in an Orthotopic Murine Model of Glioblastoma. *ACS Appl Nano Mater*. 2022;5(7):9706–9718. Copyright 2021 American Chemical Society.<sup>185</sup>

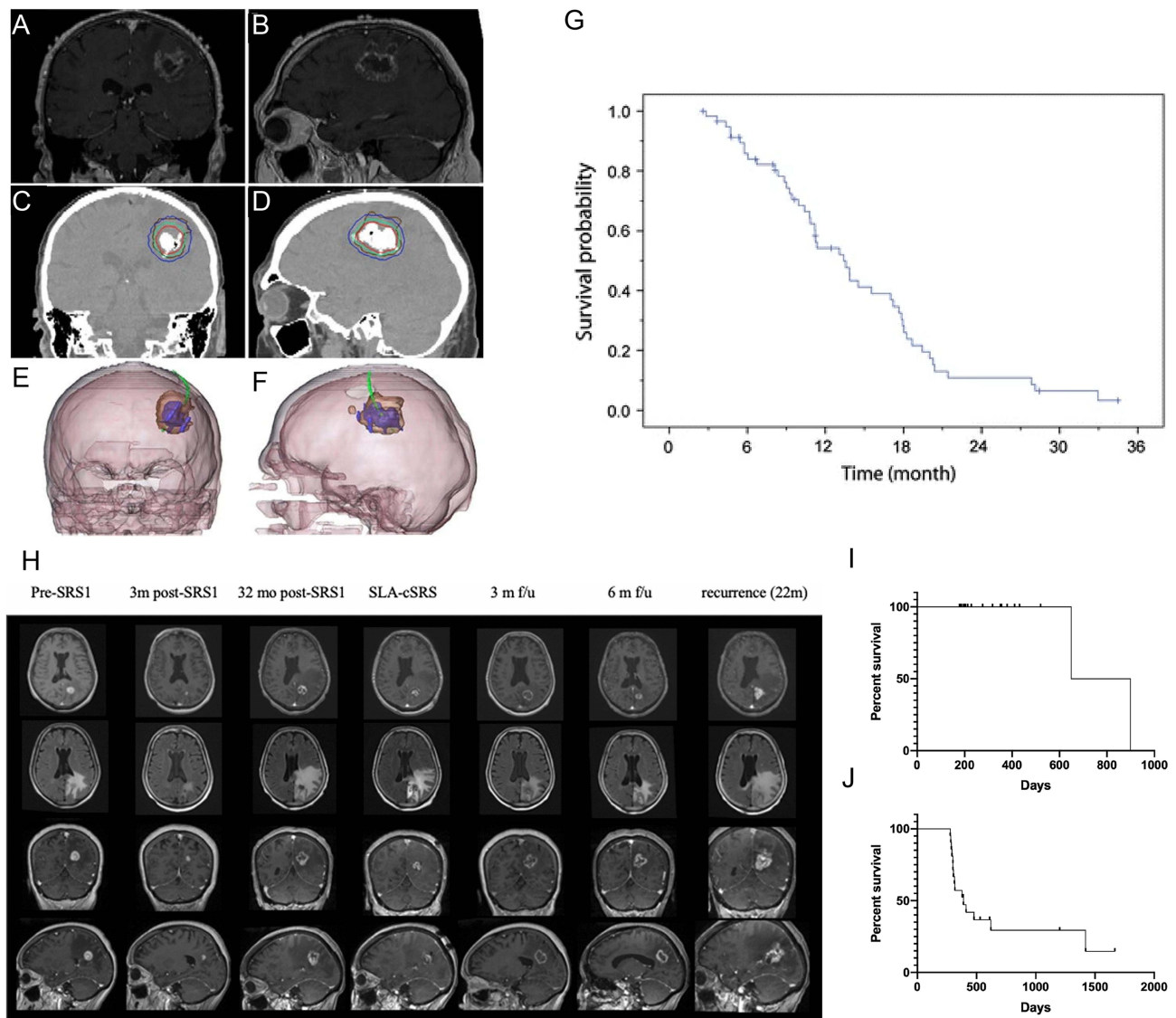


**Figure 4** (A and B) MRI before treatment. (C and D) CT imaging after the instillation of MNPs. (E and F) 3-D reconstruction of fused MRI and CT. Brown represents tumor, blue represents magnetic fluid, and green represents thermometry catheter. (G) Overall survival of patients who received treatment. (H) The sequential evolution of local recurrence for patients. (I) Local control of brain metastatic tumor after initial radiosurgery, subsequent SLA, and cSRS. (J) Overall survival of the study cohort. **Notes:** (A–G) Adapted from Maier-Hauff K, Ulrich F, Nestler D et al. Efficacy and safety of intratumoral thermotherapy using magnetic iron-oxide nanoparticles combined with external beam radiotherapy on patients with recurrent glioblastoma multiforme. *J Neurooncol.* 2011;103(2):317–324.<sup>189</sup> (H–J) Adapted with permission from Peña Pino I, Ma J, Hori YS et al. Stereotactic Laser Ablation (SLA) followed by consolidation stereotactic radiosurgery (cSRS) as treatment for brain metastasis that recurred locally after initial radiosurgery (BMRS): a multi-institutional experience. *J Neurooncol.* 2022;156(2):295–306.<sup>190</sup>

cell apoptosis but causes less damage to normal cells.<sup>193–195</sup> The induction of cell apoptosis at an iron concentration of 112 mg/mL MNPs has been employed in the treatment of glioblastoma since 2008.<sup>196</sup> Treatment at 43°C has been demonstrated to produce a therapeutic effect with mild or moderate side effects.

However, the clinical effect of pure apoptotic hyperthermia is poor, and relapse is almost always observed after therapy,<sup>197</sup> possibly because cancer cells exhibit acquired resistance to high temperatures by producing several proteins, including heat shock protein (Hsp) 90<sup>198,199</sup> and Hsp70.<sup>200–202</sup> In recent studies, MNPs have been combined with Hsp inhibitors to improve the treatment effects of apoptotic hyperthermia. Xu et al<sup>203</sup> demonstrated that 3D cells upregulate their Hsp expression to maintain cellular homeostasis at high temperatures. Therefore, it can be inferred that if Hsps are downregulated or not synthesized, cancer cells will be more sensitive to high temperatures. Hsp inhibitors have been used in thermal therapy for several tumors, including breast tumor,<sup>204,205</sup> lung cancer,<sup>206</sup> and glioblastoma multiforme.<sup>207</sup> In 2023, Wu et al<sup>208</sup> designed

a targeting modulator (AF-NPs) to recognize the CXCR4 molecule overexpressed in the BTB. This modulator released drugs to weaken the barrier function of the BTB and facilitated the transport of nanoparticles across the barrier. In another study, ZnCoFe nanoclusters (ZnCoFe NCs) were designed to co-deliver an Hsp 70 inhibitor (VER-155008) into glioblastomas. The results demonstrated the highly effective application of magnetic apoptotic hyperthermia using this system (Figure 5).

### Ultrasound Therapy Based on MNPs

Thermoablation based on MRgFUS is a promising noninvasive technique used to treat brain tumors. Compared to magnetothermal therapy, focused ultrasound thermal therapy is more economical, widely applicable, and does not require ionizing radiation. While most researchers used MRgFUS to deliver drugs into the brain based on LIFU, recent studies are increasingly exploring the use of HIFU for the direct killing of brain tumor cells.<sup>209</sup> HIFU beam can pass through soft tissues and reach the desired target without influencing normal tissues.<sup>210,211</sup> MRgFUS is a safe medical technology that has been used to treat many diseases,<sup>153</sup> including Parkinson’s disease,<sup>212</sup> obsessive-compulsive disorder,<sup>213</sup> and chronic pain.<sup>214</sup> One promising avenue for enhancing the efficacy of ultrasound thermoablation in tumor therapy involves the delivery of MNPs using focused magnetic targeting.

In 2014, Coluccia et al used a mid-frequency HIFU to treat a 63-year-old patient with glioblastoma. After 25 rounds of sonication (duration: 10–25 s; acoustic power: 150–950 W), the temperature was above 55°C. Pre- and post-MRI results indicated that HIFU permanently destroyed the tumor.<sup>215</sup> In 2022, Zhang et al<sup>216</sup> synthesized ferromagnetic Fe<sub>3</sub>O<sub>4</sub> nanoparticles with a diameter of 70 nm. The Fe<sub>3</sub>O<sub>4</sub> nanoparticles were coated onto silica after conjugation with i-motif DNA to prepare a Fe<sub>3</sub>O<sub>4</sub>@SiO<sub>2</sub>/i-motif. After the Fe<sub>3</sub>O<sub>4</sub>@SiO<sub>2</sub>/i-motif injected into the bloodstream of tumor-bearing mouse, they accumulate at the site of the tumor, and the i-motif was digested as it was sensitive to the acidic microenvironment of the tumor. The breakdown of the i-motif caused the nanoparticles to aggregate near the tumor, enhancing the MRI results and facilitating a 35% reduction in the ultrasonic power to achieve satisfactory thermal ablation (Figure 6).

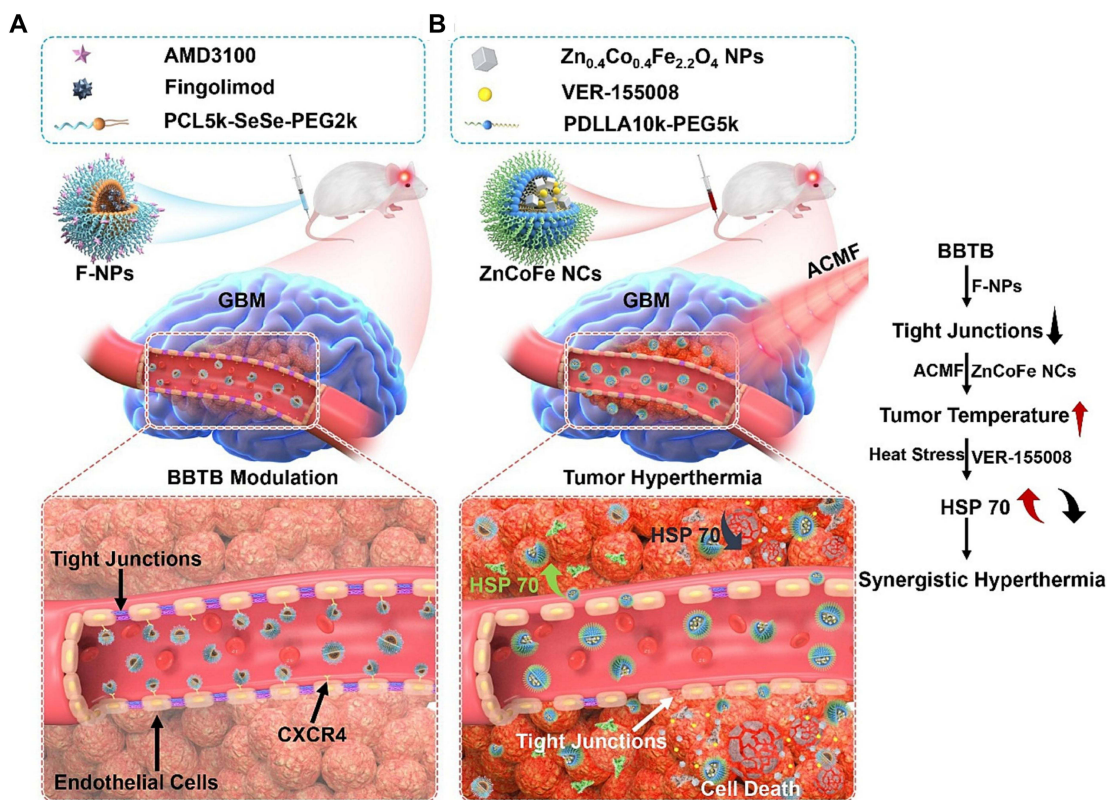


**Figure 5** Schematic diagram of magnetic apoptotic hyperthermia for glioblastoma therapy. Notes: **(A)** Construction of AF-NPs and reduction of barrier functions in the BTB. **(B)** Delivery of ZnCoFe NCs and VER-155008 to achieve highly effective magnetic apoptotic hyperthermia. Adapted from Wu H, Liu L, Ma M, Zhang Y. Modulation of blood-brain tumor barrier for delivery of magnetic hyperthermia to brain cancer. *J Control Release*. 2023;355:248–258. Copyright 2023 with permission from Elsevier.<sup>208</sup>

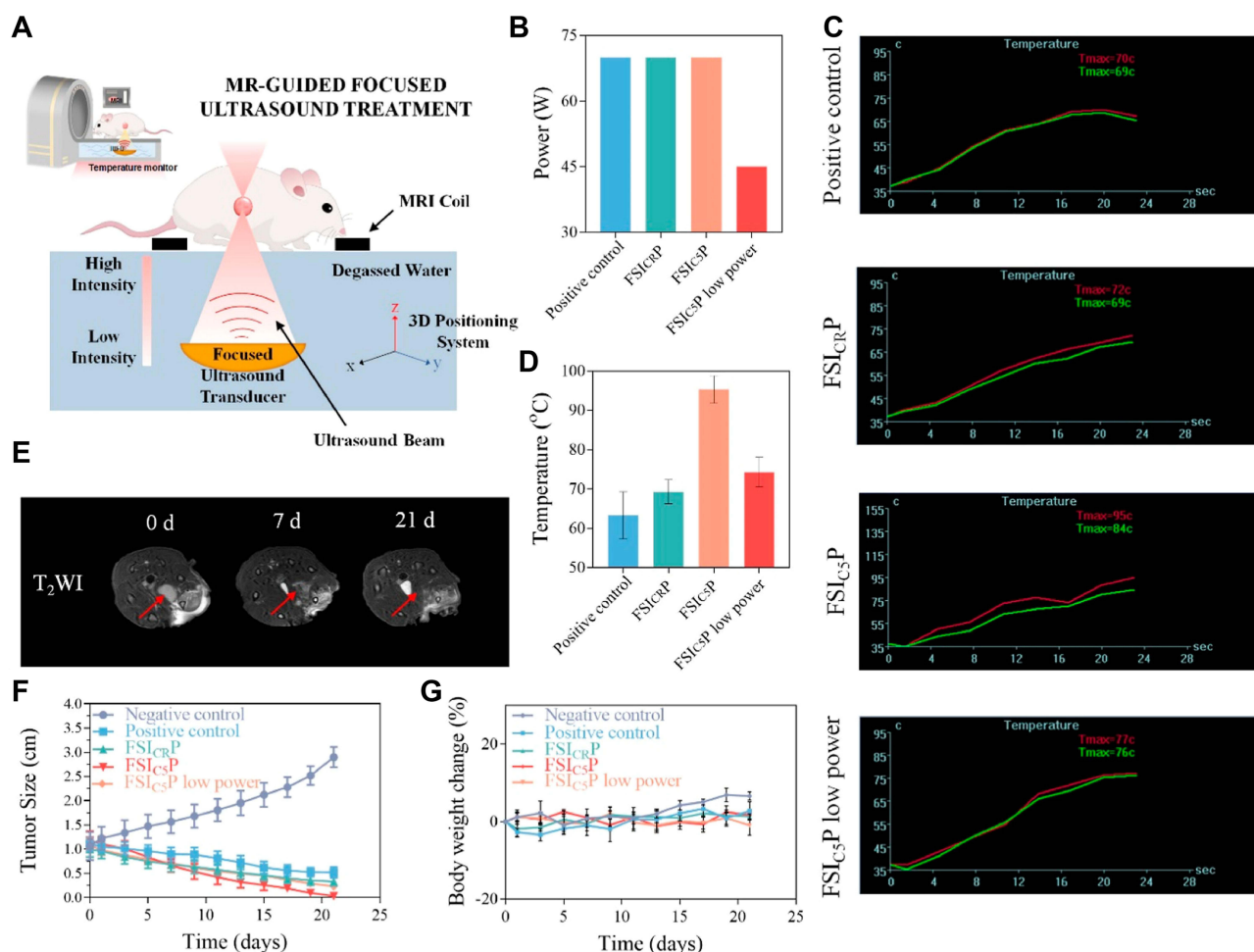


**Figure 6** Therapeutic effects of MRgFUS.

**Notes:** (A) Schematic representation of MRgFUS therapy based on the  $\text{Fe}_3\text{O}_4@\text{SiO}_2/\text{i}$ -motif. (B) Sonication energy changes in the  $\text{Fe}_3\text{O}_4@\text{SiO}_2/\text{i}$ -motif. (C) Temperature changes in the  $\text{Fe}_3\text{O}_4@\text{SiO}_2/\text{i}$ -motif. (D) Temperature after 12 h of injection with the  $\text{Fe}_3\text{O}_4@\text{SiO}_2/\text{i}$ -motif. (E) T2-weighted images at different time points after therapy. (F) Tumor size during ultrasound thermal therapy. (G) Body weight during the ultrasound thermal therapy. Adapted from Zhang X, Lu H, Tang N et al. Low-Power Magnetic Resonance-Guided Focused Ultrasound Tumor Ablation upon Controlled Accumulation of Magnetic Nanoparticles by Cascade-Activated DNA Cross-Linkers. *ACS Appl Mater Interfaces*. 2022;14(28):31677–31688. Copyright 2022 American Chemical Society.<sup>216</sup>

## Conclusion

In the past few decades, researchers have developed various delivery vectors to resolve issues related to the penetration of the BBB/BTB by anti-brain tumor drugs. Among these vectors, MNPs have emerged as the optimal choice for drug delivery to brain tumors due to their unique natural characteristics. In contrast to the limited depth at which visible spectrum and NIR light penetrate tissues, a magnetic field can easily penetrate the skull and soft tissue, enabling MNPs to achieve complete intracranial noninvasive targeted drug delivery and deep magnetothermal therapy under the influence of an EMF. Meanwhile, the deep tissue penetration ability of ultrasound, coupled with the physicochemical responses of MNPs to ultrasound, enable MNPs to achieve complete ultrasound hyperthermia under HIFU, which induces instant pore formation in the BBB/BTB to promote the transport of water-soluble drugs across the BBB/BTB into brain tumors. In addition, the nuclear magnetic resonance effect of MNPs also provides a blueprint for their application in the MRI diagnosis of brain tumors and real-time guidance of tumor dissection surgery.

Although extensive research has been conducted on the application of MNPs in the treatment of brain tumors, there are still many challenges to be addressed in clinical trials. First, it is necessary to prevent the aggregation and precipitation of MNPs to ensure their strong magnetism. Controlling the metabolic clearance of MNPs in the brain while delaying their removal by the RES system are important considerations for sustained therapeutic impact. Second,

most MNPs currently in use cannot precisely target brain cancer cells, leading to side effects. To overcome this limitation, future efforts need to focus on conjugating specific ligands (eg, antibodies, proteins, and peptides) on the surface of MNPs, allowing them to specifically recognize unique receptors on the surface of cancer cells to avoid or reduce the damage to normal cells of the CNS.

Although many difficulties will be encountered in achieving precise imaging and treatment of brain tumors using MNPs, with the rapid development of nanomedicine technology, we expect that MNPs will be widely used in the clinical treatment of brain tumors.

## Author Contributions

All authors made a significant contribution to the work reported, whether that is in the conception, study design, execution, acquisition of data, analysis and interpretation, or in all these areas; took part in drafting, revising or critically reviewing the article; gave final approval of the version to be published; have agreed on the journal to which the article has been submitted; and agree to be accountable for all aspects of the work.

## Funding

This work was supported by National Natural Science Foundation of China (82272146), Natural Science Foundation of Jilin Province (20230204048YY, 20220203124SF and YDZJ202201ZYTS252), and Norman Bethune Program of Jilin University (2022B35).

## Disclosure

The authors report no conflicts of interest in this work.

## References

1. Miller KD, Ostrom QT, Kruchko C, et al. Brain and other central nervous system tumor statistics, 2021. *CA Cancer J Clin.* 2021;71(5):381–406. doi:10.3322/caac.21693
2. Yu J, Green MD, Li S, et al. Liver metastasis restrains immunotherapy efficacy via macrophage-mediated T cell elimination. *Nat Med.* 2021;27(1):152–164. doi:10.1038/s41591-020-1131-x
3. Jabbour SK, Berman AT, Decker RH, et al. Phase 1 Trial of Pembrolizumab Administered Concurrently With Chemoradiotherapy for Locally Advanced Non–Small Cell Lung Cancer: a Nonrandomized Controlled Trial. *JAMA Oncol.* 2020;6(6):848–855. doi:10.1001/jamaoncol.2019.6731
4. Old LJ. Tumor Necrosis Factor (TNF). *Science.* 1985;230(4726):630–632. doi:10.1126/science.2413547
5. Hodi FS, O’Day SJ, McDermott DF, et al. Improved Survival with Ipilimumab in Patients with Metastatic Melanoma. *N Engl J Med.* 2010;363(8):711–723. doi:10.1056/NEJMoa1003466
6. Paz-Ares L, Luft A, Vicente D, et al. Pembrolizumab plus Chemotherapy for Squamous Non–Small-Cell Lung Cancer. *N Engl J Med.* 2018;379(21):2040–2051. doi:10.1056/NEJMoa1810865
7. Gandhi L, Rodríguez-Abreu D, Gadgeel S, et al. Pembrolizumab plus Chemotherapy in Metastatic Non–Small-Cell Lung Cancer. *N Engl J Med.* 2018;378(22):2078–2092. doi:10.1056/NEJMoa1801005
8. Adams S, Gatti-Mays ME, Kalinsky K, et al. Current Landscape of Immunotherapy in Breast Cancer: a Review. *JAMA Oncol.* 2019;5(8):1205–1214. doi:10.1001/jamaoncol.2018.7147
9. Arvanitis CD, Ferraro GB, Jain RK. The blood–brain barrier and blood–tumour barrier in brain tumours and metastases. *Nat Rev Cancer.* 2020;20(1):26–41. doi:10.1038/s41568-019-0205-x
10. Kadry H, Noorani B, Cucullo L. A blood–brain barrier overview on structure, function, impairment, and biomarkers of integrity. *Fluids Barriers CNS.* 2020;17(1):69. doi:10.1186/s12987-020-00230-3
11. Terstappen GC, Meyer AH, Bell RD, Zhang W. Strategies for delivering therapeutics across the blood–brain barrier. *Nat Rev Drug Discov.* 2021;20(5):362–383. doi:10.1038/s41573-021-00139-y
12. Tang W, Fan W, Lau J, Deng L, Shen Z, Chen X. Emerging blood–brain-barrier-crossing nanotechnology for brain cancer theranostics. *Chem Soc Rev.* 2019;48(11):2967–3014. doi:10.1039/C8CS00805A
13. Lalatsa A, Butt AM. Chapter 3 - Physiology of the Blood–Brain Barrier and Mechanisms of Transport Across the BBB. In: Kesharwani P, Gupta U, editors. *Nanotechnology-Based Targeted Drug Delivery Systems for Brain Tumors.* Academic Press; 2018:49–74.
14. Huang J, Li Y, Orza A, et al. Magnetic Nanoparticle Facilitated Drug Delivery for Cancer Therapy with Targeted and Image-Guided Approaches. *Adv Funct Mater.* 2016;26(22):3818–3836. doi:10.1002/adfm.201504185
15. Li B, Chen X, Qiu W, et al. Synchronous Disintegration of Ferroptosis Defense Axis via Engineered Exosome-Conjugated Magnetic Nanoparticles for Glioblastoma Therapy. *Adv Sci.* 2022;9(17):2105451. doi:10.1002/advs.202105451
16. Zhang J, Zhang T, Gao J. Biocompatible Iron Oxide Nanoparticles for Targeted Cancer Gene Therapy: a Review. *Nanomaterials.* 2022;12(19):3323. doi:10.3390/nano12193323
17. Cao Y, Zhang S, Ma M, Zhang Y. Fluorinated PEG-PEI Coated Magnetic Nanoparticles for siRNA Delivery and CXCR4 Knockdown. *Nanomaterials.* 2022;12(10):1692. doi:10.3390/nano12101692

18. Han H, Hou Y, Chen X, et al. Metformin-Induced Stromal Depletion to Enhance the Penetration of Gemcitabine-Loaded Magnetic Nanoparticles for Pancreatic Cancer Targeted Therapy. *J Am Chem Soc.* 2020;142(10):4944–4954. doi:10.1021/jacs.0c00650
19. Guo Y, Ran Y, Wang Z, et al. Magnetic-responsive and targeted cancer nanotheranostics by PA/MR bimodal imaging-guided photothermally triggered immunotherapy. *Biomaterials.* 2019;219:119370. doi:10.1016/j.biomaterials.2019.119370
20. Ma Y, Yan C, Guo Z, et al. Spatio-Temporally Reporting Dose-Dependent Chemotherapy via Uniting Dual-Modal MRI/NIR Imaging. *Angew Chem Int Ed.* 2020;59(47):21143–21150. doi:10.1002/anie.202009380
21. Song G, Kenney M, Chen Y-S, et al. Carbon-coated FeCo nanoparticles as sensitive magnetic-particle-imaging tracers with photothermal and magnetothermal properties. *Nat Biomed Eng.* 2020;4(3):325–334. doi:10.1038/s41551-019-0506-0
22. Huang G, Qiu Y, Yang F, et al. Magnetothermally Triggered Free-Radical Generation for Deep-Seated Tumor Treatment. *Nano Lett.* 2021;21(7):2926–2931. doi:10.1021/acs.nanolett.1c00009
23. Pan J, Xu Y, Wu Q, Hu P, Shi J. Mild Magnetic Hyperthermia-Activated Innate Immunity for Liver Cancer Therapy. *J Am Chem Soc.* 2021;143(21):8116–8128. doi:10.1021/jacs.1c02537
24. Sadeghi-Goughari M, Jeon S, Kwon H-J. Magnetic nanoparticles-enhanced focused ultrasound heating: size effect, mechanism, and performance analysis. *Nanotechnology.* 2020;31(24):245101. doi:10.1088/1361-6528/ab7cea
25. Liu H-L, Hua M-Y, Yang H-W, et al. Magnetic resonance monitoring of focused ultrasound/magnetic nanoparticle targeting delivery of therapeutic agents to the brain. *Proc Natl Acad Sci.* 2010;107(34):15205–15210. doi:10.1073/pnas.1003388107
26. Torres-Díaz I, Rinaldi C. Recent progress in ferrofluids research: novel applications of magnetically controllable and tunable fluids. *Soft Matter.* 2014;10(43):8584–8602. doi:10.1039/C4SM01308E
27. Tong S, Zhu H, Bao G. Magnetic iron oxide nanoparticles for disease detection and therapy. *Mater Today.* 2019;31:86–99. doi:10.1016/j.mattod.2019.06.003
28. Paunovic J, Vucevic D, Radosavljevic T, Mandić-Rajčević S, Pantic I. Iron-based nanoparticles and their potential toxicity: focus on oxidative stress and apoptosis. *Chem Biol Interact.* 2020;316:108935. doi:10.1016/j.cbi.2019.108935
29. Huber DL. Synthesis, Properties, and Applications of Iron Nanoparticles. *Small.* 2005;1(5):482–501. doi:10.1002/sml.200500006
30. Hou Y, Gao S. Monodisperse nickel nanoparticles prepared from a monosurfactant system and their magnetic properties. *J Mater Chem.* 2003;13(7):1510–1512. doi:10.1039/B303226D
31. Cordente N, Respaud M, Senocq F, Casanove M-J, Amiens C, Chaudret B. Synthesis and Magnetic Properties of Nickel Nanorods. *Nano Lett.* 2001;1(10):565–568. doi:10.1021/nl0100522
32. Başkaya G, Yıldız Y, Savk A, et al. Rapid, sensitive, and reusable detection of glucose by highly monodisperse nickel nanoparticles decorated functionalized multi-walled carbon nanotubes. *Biosens Bioelectron.* 2017;91:728–733. doi:10.1016/j.bios.2017.01.045
33. Gomaji Chaudhary R, Tanna A, J G. Synthesis Of Nickel Nanoparticles: microscopic Investigation, An Efficient Catalyst And Effective Antibacterial Activity. *Adv Mater Lett.* 2015;6(11):990–998. doi:10.5185/amlett.2015.5901
34. Shukla V, Jayabalan J, Chari R. Optical shielding of nickel nanoparticle by a bubble: optical limiting gets limited. *Appl Phys Lett.* 2016;108(24):567.
35. Liu F, Ma G, Zhao D. Nickel nanoparticle-stabilized room-temperature blue-phase liquid crystals. *Nanotechnology.* 2018;29(28):285703. doi:10.1088/1361-6528/aabaa4
36. Metin Ö, Mazumder V, Özkaz S, Sun S. Monodisperse Nickel Nanoparticles and Their Catalysis in Hydrolytic Dehydrogenation of Ammonia Borane. *J Am Chem Soc.* 2010;132(5):1468–1469. doi:10.1021/ja909243z
37. Park J, Kang E, Son SU, et al. Monodisperse Nanoparticles of Ni and NiO: synthesis, Characterization, Self-Assembled Superlattices, and Catalytic Applications in the Suzuki Coupling Reaction. *Adv Mater.* 2005;17(4):429–434. doi:10.1002/adma.200400611
38. Guo K, Li H, Yu Z. Size-Dependent Catalytic Activity of Monodispersed Nickel Nanoparticles for the Hydrolytic Dehydrogenation of Ammonia Borane. *ACS Appl Mater Interfaces.* 2018;10(1):517–525. doi:10.1021/acsami.7b14166
39. Samia AC, Hyzer K, Schlueter JA, et al. Ligand effect on the growth and the digestion of Co nanocrystals. *J Am Chem Soc.* 2005;127(12):4126–4127.
40. Fuller RO, Goh B-M, Koutsantonis GA, Loedolff MJ, Saunders M, Woodward RC. A simple procedure for the production of large ferromagnetic cobalt nanoparticles. *Dalton Trans.* 2016;45(30):11983–11989. doi:10.1039/c6dt01935h
41. Psimadas D, Baldi G, Ravagli C, et al. Comparison of the magnetic, radiolabeling, hyperthermic and biodistribution properties of hybrid nanoparticles bearing CoFe<sub>2</sub>O<sub>4</sub> and Fe<sub>3</sub>O<sub>4</sub> metal cores. *Nanotechnology.* 2014;25(2):025101. doi:10.1088/0957-4484/25/2/025101
42. Bjørnerud A, Briley-Sæbø K, Johansson LO, Kellar KE. Effect of NC100150 injection on the 1H NMR linewidth of human whole blood ex vivo: dependency on blood oxygen tension. *Magn Reson Med.* 2000;44(5):803–807. doi:10.1002/1522-2594(200011)44:5<803::AID-MRM19>3.0.CO;2-K
43. Du V, Luciani N, Richard S, et al. A 3D magnetic tissue stretcher for remote mechanical control of embryonic stem cell differentiation. *Article Nat Commun.* 2017;8(1):400. doi:10.1038/s41467-017-00543-2
44. Petrarca C, Poma AM, Vecchiotti G, et al. Cobalt magnetic nanoparticles as theranostics: conceivable or forgettable?. *Nanotechn Rev.* 2020;9(1):1522–1538. doi:10.1515/ntrev-2020-0111
45. Hu R, Dai C, Dai X, et al. Topology regulation of nanomedicine for autophagy-augmented ferroptosis and cancer immunotherapy. *Sci Bull.* 2023;68(1):77–94. doi:10.1016/j.scib.2022.12.030
46. Giltinan J, Sridhar V, Bozuyuk U, Sheehan D, Sitti M. 3D Microprinting of Iron Platinum Nanoparticle-Based Magnetic Mobile Microrobots. *Adv Intell Syst.* 2021;3(1):2000204. doi:10.1002/aisy.202000204
47. Chang Z-X, C-H L, Chang Y-C, Huang C-YF, Chan M-H, Hsiao M. Novel monodisperse FePt nanocomposites for T2-weighted magnetic resonance imaging: biomedical theranostics applications. *Nanoscale Adv.* 2022;4(2):377–386. doi:10.1039/D1NA00613D
48. Céspedes MV, Unzueta U, Tatkievicz W, et al. In Vivo Architectonic Stability of Fully de Novo Designed Protein-Only Nanoparticles. *ACS Nano.* 2014;8(5):4166–4176. doi:10.1021/nn405573z
49. Kekalo K, Shubitidze F, Meyers R, Yaqub R, Baker I. Magnetic Heating of Fe-Co Ferrites — experiments and Modeling. *Nano LIFE.* 2016;06(02):1650007. doi:10.1142/s1793984416500070
50. Wang C, Hsu C-H, Li Z, et al. Effective heating of magnetic nanoparticle aggregates for in vivo nano-theranostic hyperthermia. *Int J Nanomed.* 2017;12:6273–6287. doi:10.2147/IJN.S141072
51. Huang K, Li Z, Lin J, Han G, Huang P. Two-dimensional transition metal carbides and nitrides (MXenes) for biomedical applications. *Chem Soc Rev.* 2018;47(14):5109–5124. doi:10.1039/C7CS00838D

52. Yang W, Rehman S, Chu X, Hou Y, Gao S. Transition Metal (Fe, Co and Ni) Carbide and Nitride Nanomaterials: structure, Chemical Synthesis and Applications. *ChemNanoMat*. 2015;1(6):376–398. doi:10.1002/cnma.201500073
53. Lee N, Yoo D, Ling D, Cho MH, Hyeon T, Cheon J. Iron Oxide Based Nanoparticles for Multimodal Imaging and Magneto-responsive Therapy. *Chem Rev*. 2015;115(19):10637–10689. doi:10.1021/acs.chemrev.5b00112
54. Au - Castaneda RT, Au - Khurana A, Au - Khan R. Labeling Stem Cells with Ferumoxytol, an FDA-Approved Iron Oxide Nanoparticle. *J Vis Exp*. 2011;57:e3482. doi:10.3791/3482
55. Korangath P, Barnett JD, Sharma A, et al. Nanoparticle interactions with immune cells dominate tumor retention and induce T cell-mediated tumor suppression in models of breast cancer. *Sci Adv*. 2020;6(13):eaay1601. doi:10.1126/sciadv.aay1601
56. Gemici C, Yetmen O, Yaprak G, et al. Is there any role of intravenous iron for the treatment of anemia in cancer?. *BMC Cancer*. 2016;16(1):661. doi:10.1186/s12885-016-2686-2
57. Zanganeh S, Hutter G, Spitzer R, et al. Iron oxide nanoparticles inhibit tumour growth by inducing pro-inflammatory macrophage polarization in tumour tissues. *Nat Nanotechnol*. 2016;11(11):986–994. doi:10.1038/nnano.2016.168
58. Lebrun F, Klustersky J, Levacq D, Wissam Y, Paesmans M. Intravenous iron therapy for anemic cancer patients: a review of recently published clinical studies. *Support Care Cancer*. 2017;25(7):2313–2319. doi:10.1007/s00520-017-3672-1
59. Baribeault D, Auerbach M. Iron replacement therapy in cancer-related anemia. *Am J Health Syst Pharm*. 2011;68(10\_Supplement\_1):S4–S14. doi:10.2146/ajhp110039
60. Kalska-Szoszko B, Wykowska U, Satała D. Magnetic nanoparticles of core-shell structure. *Colloids Surf A: Physicochem Eng Aspects*. 2015;481:527–536. doi:10.1016/j.colsurfa.2015.05.040
61. Hong RY, Zhang SZ, Di GQ, et al. Preparation, characterization and application of Fe<sub>3</sub>O<sub>4</sub>/ZnO core/shell magnetic nanoparticles. *Mater Res Bull*. 2008;43(8):2457–2468. doi:10.1016/j.materresbull.2007.07.035
62. Chen W-J, Tsai P-J, Chen Y-C. Functional Fe<sub>3</sub>O<sub>4</sub>/TiO<sub>2</sub> Core/Shell Magnetic Nanoparticles as Photokilling Agents for Pathogenic Bacteria. *Small*. 2008;4(4):485–491. doi:10.1002/sml.200701164
63. Cui Y-R, Hong C, Zhou Y-L, Li Y, Gao X-M, Zhang X-X. Synthesis of orientedly bioconjugated core/shell Fe<sub>3</sub>O<sub>4</sub>@Au magnetic nanoparticles for cell separation. *Talanta*. 2011;85(3):1246–1252. doi:10.1016/j.talanta.2011.05.010
64. Martín M, Salazar P, Villalonga R, Campuzano S, Pingarrón JM, González-Mora JL. Preparation of core-shell Fe<sub>3</sub>O<sub>4</sub>@poly(dopamine) magnetic nanoparticles for biosensor construction. *J Mater Chem B*. 2014;2(6):739–746. doi:10.1039/C3TB21171A
65. Shi D, Yang H, Ji S, Jiang S, Liu X, Zhang D. Preparation and Characterization of Core-shell Structure Fe<sub>3</sub>O<sub>4</sub>@C Magnetic Nanoparticles. *Procedia Eng*. 2015;102:1555–1562. doi:10.1016/j.proeng.2015.01.291
66. Teo SH, Islam A, Chan ES, et al. Efficient biodiesel production from *Jatropha curcus* using CaSO<sub>4</sub>/Fe<sub>2</sub>O<sub>3</sub>-SiO<sub>2</sub> core-shell magnetic nanoparticles. *J Clean Prod*. 2019;208:816–826. doi:10.1016/j.jclepro.2018.10.107
67. Zomorodian K, Veisi H, Mousavi SM, et al. Modified magnetic nanoparticles by PEG-400-immobilized Ag nanoparticles (Fe<sub>3</sub>O<sub>4</sub>@PEG-Ag) as a core/shell nanocomposite and evaluation of its antimicrobial activity. *Int J Nanomed*. 2018;13:3965–3973. doi:10.2147/IJN.S161002
68. Liu Y, Yang K, Cheng L, et al. PEGylated FePt@Fe<sub>2</sub>O<sub>3</sub> core-shell magnetic nanoparticles: potential theranostic applications and in vivo toxicity studies. *Nanomed Nanotechnol Biol Med*. 2013;9(7):1077–1088. doi:10.1016/j.nano.2013.02.010
69. Yang S, Zong P, Ren X, Wang Q, Wang X. Rapid and Highly Efficient Preconcentration of Eu(III) by Core-Shell Structured Fe<sub>3</sub>O<sub>4</sub>@Humic Acid Magnetic Nanoparticles. *ACS Appl Mater Interfaces*. 2012;4(12):6891–6900. doi:10.1021/am3020372
70. Estrader M, López-Ortega A, Estradé S, et al. Robust antiferromagnetic coupling in hard-soft bi-magnetic core/shell nanoparticles. *Nat Commun*. 2013;4(1):2960. doi:10.1038/ncomms3960
71. G-y L, Jiang Y-R, Huang K-L, Ding P, Chen J. Preparation and properties of magnetic Fe<sub>3</sub>O<sub>4</sub>-chitosan nanoparticles. *J Alloys Compd*. 2008;466(1–2):56. doi:10.1016/j.jallcom.2007.11.100
72. Suleman M, Riaz S. In silico study of hyperthermia treatment of liver cancer using core-shell CoFe<sub>2</sub>O<sub>4</sub>@ MnFe<sub>2</sub>O<sub>4</sub> magnetic nanoparticles. *J Magn Magn Mater*. 2020;498:166143. doi:10.1016/j.jmmm.2019.166143
73. Wang Y, Gu H. Core-Shell-Type Magnetic Mesoporous Silica Nanocomposites for Bioimaging and Therapeutic Agent Delivery. *Adv Mater*. 2015;27(3):576–585. doi:10.1002/adma.201401124
74. Wu J, Hou Y, Gao S. Controlled synthesis and multifunctional properties of FePt-Au heterostructures. *Nano Res*. 2011;4(9):836–848. doi:10.1007/s12274-011-0140-y
75. Zhu J, Wu J, Liu F, et al. Controlled synthesis of FePt-Au hybrid nanoparticles triggered by reaction atmosphere and FePt seeds. *Nanoscale*. 2013;5(19):9141–9149. doi:10.1039/C3NR02911E
76. Kong M, Jia Z, Wang B, et al. Construction of metal-organic framework derived Co/ZnO/Ti<sub>3</sub>C<sub>2</sub>T<sub>x</sub> composites for excellent microwave absorption. *Sustainable Mater Technol*. 2020;26:e00219. doi:10.1016/j.susmat.2020.e00219
77. Feng W, Liu Y, Bi Y, et al. Recent advancement of magnetic MOF composites in microwave absorption. *Synth Met*. 2023;294:117307. doi:10.1016/j.synthmet.2023.117307
78. Pukdeejorhor L, Adpakpang K, Ponchai P, et al. Polymorphism of Mixed Metal Cr/Fe Terephthalate Metal-Organic Frameworks Utilizing a Microwave Synthetic Method. *Cryst Growth Des*. 2019;19(10):5581–5591. doi:10.1021/acs.cgd.9b00508
79. Chen H, Hong R, Liu Q, et al. CNFs@carbonaceous Co/CoO composite derived from CNFs penetrated through ZIF-67 for high-efficient electromagnetic wave absorption material. *J Alloys Compd*. 2018;752:115–122. doi:10.1016/j.jallcom.2018.04.142
80. Zeng Q, Wang L, Li X, et al. Double ligand MOF-derived pomegranate-like Ni@C microspheres as high-performance microwave absorber. *Appl Surf Sci*. 2021;538:148051. doi:10.1016/j.apsusc.2020.148051
81. Shu R, Li N, Li X, Sun J. Preparation of FeNi/C composite derived from metal-organic frameworks as high-efficiency microwave absorbers at ultrathin thickness. *J Colloid Interface Sci*. 2022;606:1918–1927. doi:10.1016/j.jcis.2021.10.011
82. Lin K, Wu L, Wu T, et al. Bimetal-doped core-shell carbon derived from nickel-cobalt dual-ligand metal-organic framework for adjustable strong microwave absorption. *J Colloid Interface Sci*. 2022;627:90–101. doi:10.1016/j.jcis.2022.07.048
83. Hu Q, Yang R, Yang S, Huang W, Zeng Z, Gui X. Metal-Organic Framework-Derived Core-Shell Nanospheres Anchored on Fe-Filled Carbon Nanotube Sponge for Strong Wideband Microwave Absorption. *ACS Appl Mater Interfaces*. 2022;14(8):10577–10587. doi:10.1021/acsami.1c25019



84. Ebrahimpour A, Riahi Alam N, Abdolmaleki P, et al. Magnetic Metal–Organic Framework Based on Zinc and 5-Aminolevulinic Acid: MR Imaging and Brain Tumor Therapy. *J Inorg Organomet Polym Mater.* 2021;31(3):1208–1216. doi:10.1007/s10904-020-01782-5
85. Li Z, Wang C, Chen J, et al. uPAR targeted phototheranostic metal-organic framework nanoprobe for MR/NIR-II imaging-guided therapy and surgical resection of glioblastoma. *Mater Design.* 2021;198:109386. doi:10.1016/j.matdes.2020.109386
86. Reddy LH, Arias JL, Nicolas J, Couvreur P. Magnetic Nanoparticles: design and Characterization, Toxicity and Biocompatibility, Pharmaceutical and Biomedical Applications. *Chem Rev.* 2012;112(11):5818–5878. doi:10.1021/cr300068p
87. Wang X, Zhuang J, Peng Q, Li Y. A general strategy for nanocrystal synthesis. *Nature.* 2005;437(7055):121–124. doi:10.1038/nature03968
88. Rafie SF, Sayahi H, Abdollahi H, Abu-Zahra N. Hydrothermal synthesis of Fe<sub>3</sub>O<sub>4</sub> nanoparticles at different pHs and its effect on discoloration of methylene blue: evaluation of alternatives by TOPSIS method. *Mater Today Commun.* 2023;37:107589. doi:10.1016/j.mtcomm.2023.107589
89. Mohamed AE-MA, Mohamed MA. Nanoparticles: magnetism and Applications. In: Abd-Elsalam KA, Mohamed MA, Prasad R, editors. *Magnetic Nanostructures : Environmental and Agricultural Applications.* Springer International Publishing; 2019:1–12.
90. Kudr J, Haddad Y, Richtera L, et al. Magnetic Nanoparticles: from Design and Synthesis to Real World Applications. *Nanomaterials.* 2017;7(9):243. doi:10.3390/nano7090243
91. Insausti M. Tuning the composition of multidoped magnetite nanoparticles starting from bimetallic FeMn, FeCo and FeZn oleates.
92. Ali A, Shah T, Ullah R, et al. Review on Recent Progress in Magnetic Nanoparticles: synthesis, Characterization, and Diverse Applications. *Review Front Chem.* 2021;9. doi:10.3389/fchem.2021.629054
93. Chen JP, Sorensen CM, Klabunde KJ, Hadjipanayis GC, Devlin E, Kostikas A. Size-dependent magnetic properties of MnFe<sub>2</sub>O<sub>4</sub> fine particles synthesized by coprecipitation. *Phys Rev B.* 1996;54(13):9288–9296. doi:10.1103/PhysRevB.54.9288
94. Chen Q, Rondinone AJ, Chakoumakos C, John Zhang B. Synthesis of superparamagnetic MgFe<sub>2</sub>O<sub>4</sub> nanoparticles by coprecipitation. *J Magn Magn Mater.* 1999;194(1):1–7. doi:10.1016/S0304-8853(98)00585-X
95. Mireles L-K, Sacher E, Yahia LH, Laurent S, Stanicki D. A comparative physicochemical, morphological and magnetic study of silane-functionalized superparamagnetic iron oxide nanoparticles prepared by alkaline coprecipitation. *INT J BIOCHEM CELL B.* 2016;75:203–211. doi:10.1016/j.biocel.2015.12.002
96. Park J, An K, Hwang Y, et al. Ultra-large-scale syntheses of monodisperse nanocrystals. *Nat Mater.* 2004;3(12):891–895. doi:10.1038/nmat1251
97. de Mello LB, Varanda LC, Sigoli FA, Mazali IO. Co-precipitation synthesis of (Zn-Mn)-co-doped magnetite nanoparticles and their application in magnetic hyperthermia. *J Alloys Compd.* 2019;779:698–705. doi:10.1016/j.jallcom.2018.11.280
98. Andrade RGD, Veloso SRS, Castanheira EMS. Shape Anisotropic Iron Oxide-Based Magnetic Nanoparticles: synthesis and Biomedical Applications. *Int J Mol Sci.* 2020;21(7). doi:10.3390/ijms21072455
99. Ait Kerroum MA, Essyed A, Iacovita C, et al. The effect of basic pH on the elaboration of ZnFe<sub>2</sub>O<sub>4</sub> nanoparticles by co-precipitation method: structural, magnetic and hyperthermia characterization. *J Magn Magn Mater.* 2019;478:239–246. doi:10.1016/j.jmmm.2019.01.081
100. Masunga N, Mamba BB, Getahun YW, El-Gendy AA, Kefeni KK. Synthesis of single-phase superparamagnetic copper ferrite nanoparticles using an optimized coprecipitation method. *Materials Sci Eng.* 2021;272:115368. doi:10.1016/j.mseb.2021.115368
101. Biehl P, Von der Lühe M, Dutz S, Schacher FH. Synthesis, Characterization, and Applications of Magnetic Nanoparticles Featuring Polyzwitterionic Coatings. *Polymers.* 2018;10(1):91. doi:10.3390/polym10010091
102. Shan D, Deng S, Zhao T, et al. Preparation of ultrafine magnetic biochar and activated carbon for pharmaceutical adsorption and subsequent degradation by ball milling. *J Hazard Mater.* 2016;305:156–163. doi:10.1016/j.jhazmat.2015.11.047
103. Lerner MI, Glazkova EA, Lozhkomoev AS, et al. Synthesis of Al nanoparticles and Al/AlN composite nanoparticles by electrical explosion of aluminum wires in argon and nitrogen. *Powder Technol.* 2016;295:307–314. doi:10.1016/j.powtec.2016.04.005
104. Jendrzey S, Gökce B, Epple M, Barcikowski S. How Size Determines the Value of Gold: economic Aspects of Wet Chemical and Laser-Based Metal Colloid Synthesis. *ChemPhysChem.* 2017;18(9):1012–1019. doi:10.1002/cphc.201601139
105. Kotov YA. Electric Explosion of Wires as a Method for Preparation of Nanopowders. *J Nanopart Res.* 2003;5(5):539–550. doi:10.1023/B:NANO.000006069.45073.0b
106. Kawamura G, Alvarez S, Stewart IE, Catenacci M, Chen Z, Ha Y-C. Production of Oxidation-Resistant Cu-Based Nanoparticles by Wire Explosion. *Sci Rep.* 2015;5(1):18333. doi:10.1038/srep18333
107. Komeili A. Molecular mechanisms of compartmentalization and biomineralization in magnetotactic bacteria. *FEMS Microbiol Rev.* 2012;36(1):232–255. doi:10.1111/j.1574-6976.2011.00315.x
108. Gul S, Khan SB, Rehman IU, Khan MA, Khan MI. A Comprehensive Review of Magnetic Nanomaterials Modern Day Theranostics. *Review Front Mater.* 2019;6. doi:10.3389/fmats.2019.00179
109. Abhilash RK, Pandey BD. Microbial synthesis of iron-based nanomaterials—A review. *Bull Mater Sci.* 2011;34(2):191–198. doi:10.1007/s12034-011-0076-6
110. Makarov VV, Makarova SS, Love AJ, et al. Biosynthesis of stable iron oxide nanoparticles in aqueous extracts of *Hordeum vulgare* and *Rumex acetosa* plants. *Langmuir.* 2014;30(20):5982–5988. doi:10.1021/la501192a
111. Kumar B, Smita K, Cumbal L, Debut A, Galeas S, Guerrero VH. Phytosynthesis and photocatalytic activity of magnetite (Fe<sub>3</sub>O<sub>4</sub>) nanoparticles using the Andean blackberry leaf. *Mater Chem Phys.* 2016;179:310–315. doi:10.1016/j.matchemphys.2016.05.045
112. Hsu C-Y, F-Y K, C-W L, Fann K, Lue J-T. Magnetoreception System in Honeybees (*Apis mellifera*). *PLoS One.* 2007;2(4):e395. doi:10.1371/journal.pone.0000395
113. Saaduldeen Anwer S. Simultaneous green synthesis of Magnetite-Nanoparticles MNPs using microalgae *Spirulina sp.* for antibacterial activity. *Emirates Journal of Food and Agriculture.* 2023;35(4):56. doi:10.9755/ejfa.2023.v35.i4.3033
114. El-Sesy ME, Othman SA. Promising antibacterial activities of anethole and green-synthesized magnetite nanoparticles against multiple antibiotic-resistant bacteria. *Water Sci Technol.* 2023;87(3):729–747. doi:10.2166/wst.2023.012
115. Furlani EP, Ng KC. Nanoscale magnetic biotransport with application to magnetofection. *Phys Rev E.* 2008;77(6):061914. doi:10.1103/PhysRevE.77.061914
116. Dobson J. Remote control of cellular behaviour with magnetic nanoparticles. *Nat Nanotechnol.* 2008;3(3):139–143. doi:10.1038/nnano.2008.39
117. Mannix RJ, Kumar S, Cassiola F, et al. Nanomagnetic actuation of receptor-mediated signal transduction. *Nat Nanotechnol.* 2008;3(1):36–40. doi:10.1038/nnano.2007.418

118. Qiu Y, Tong S, Zhang L, et al. Magnetic forces enable controlled drug delivery by disrupting endothelial cell-cell junctions. *Nat Commun.* 2017;8(1):15594. doi:10.1038/ncomms15594
119. Weissleder R, Elizondo G, Wittenberg J, Rabito CA, Bengel HH, Josephson L. Ultrasmall superparamagnetic iron oxide: characterization of a new class of contrast agents for MR imaging. *Radiology.* 1990;175(2):489–493. doi:10.1148/radiology.175.2.2326474
120. Lewin M, Carlesso N, Tung C-H, et al. Tat peptide-derivatized magnetic nanoparticles allow in vivo tracking and recovery of progenitor cells. *Nat Biotechnol.* 2000;18(4):410–414. doi:10.1038/74464
121. Gilchrist RK, Medal R, Shorey WD, Hanselman RC, Parrott JC, Taylor CB. Selective Inductive Heating of Lymph Nodes. *Ann Surg.* 1957;146(4):596–606. doi:10.1097/00000658-195710000-00007
122. Li Y, Bao Q, Yang S, Yang M, Mao C. Bionanoparticles in cancer imaging, diagnosis, and treatment. *View.* 2022;3(4):20200027. doi:10.1002/VIW.20200027
123. Maeda H, Nakamura H, Fang J. The EPR effect for macromolecular drug delivery to solid tumors: improvement of tumor uptake, lowering of systemic toxicity, and distinct tumor imaging in vivo. *Adv Drug Deliv Rev.* 2013;65(1):71–79. doi:10.1016/j.addr.2012.10.002
124. Sindhwani S, Syed AM, Ngai J, et al. The entry of nanoparticles into solid tumours. *Nat Mater.* 2020;19(5):566–575. doi:10.1038/s41563-019-0566-2
125. Wang X, Chang Y, Zhang D, Tian B, Yang Y, Wei F. Transferrin-conjugated drug/dye-co-encapsulated magnetic nanocarriers for active-targeting fluorescent/magnetic resonance imaging and anti-tumor effects in human brain tumor cells. *Rsc Adv.* 2016;6(107):105661–105675. doi:10.1039/C6RA20903C
126. Singh R, Norret M, House MJ, et al. Dose-Dependent Therapeutic Distinction between Active and Passive Targeting Revealed Using Transferrin-Coated PGMA Nanoparticles. *Small.* 2016;12(3):351–359. doi:10.1002/smll.201502730
127. Ghadiri M, Vasheghani-Farahani E, Atyabi F, Kobarfard F, Mohamadyar-Toupkanlou F, Hosseinkhani H. Transferrin-conjugated magnetic dextran-spermine nanoparticles for targeted drug transport across blood-brain barrier. *J Biomed Mater Res Part A.* 2017;105(10):2851–2864. doi:10.1002/jbm.a.36145
128. Song B, Jiang J, Yan H, Huang S, Yuan J. A tumor-targetable probe based on europium(iii)/gadolinium(iii) complex-conjugated transferrin for dual-modal time-gated luminescence and magnetic resonance imaging of cancerous cells in vitro and in vivo. *J Mater Chem B.* 2023;11(19):4346–4353. doi:10.1039/D3TB00387F
129. Villalobos-Manzo R, Rios-Castro E, Hernández-Hernández JM, Oza G, Medina MA, Tapia-Ramírez J. Identification of Transferrin Receptor 1 (TfR1) Overexpressed in Lung Cancer Cells, and Internalization of Magnetic Au-CoFe<sub>2</sub>O<sub>4</sub> Core-Shell Nanoparticles Functionalized with Its Ligand in a Cellular Model of Small Cell Lung Cancer (SCLC). *Pharmaceutics.* 2022;14(8):1715. doi:10.3390/pharmaceutics14081715
130. Ge P, Liu Y, Chen Q, et al. Transferrin receptors/magnetic resonance dual-targeted nanoplatfor for precise chemo-photodynamic synergistic cancer therapy. *Nanomed Nanotechnol Biol Med.* 2022;39:102467. doi:10.1016/j.nano.2021.102467
131. Pan Y, Wang Z, Ma J, et al. Folic Acid-Modified Fluorescent-Magnetic Nanoparticles for Efficient Isolation and Identification of Circulating Tumor Cells in Ovarian Cancer. *Biosensors.* 2022;12(3):184. doi:10.3390/bios12030184
132. Derakhshankhah H, Haghshenas B, Eskandani M, Jahanban-Esfahlan R, Abbasi-Maleki S, Jaymand M. Folate-conjugated thermal- and pH-responsive magnetic hydrogel as a drug delivery nano-system for “smart” chemo/hyperthermia therapy of solid tumors. *Mater Today Commun.* 2022;30:103148. doi:10.1016/j.mtcomm.2022.103148
133. Wang Q, Cheng Y, Wang W, Tang X, Yang Y. Polyetherimide- and folic acid-modified Fe<sub>3</sub>O<sub>4</sub> nanospheres for enhanced magnetic hyperthermia performance. *J Biomed Mater Res B Appl Biomater.* 2023;111(4):795–804. doi:10.1002/jbm.b.35190
134. Hong JY, Lim YG, Song YJ, Park K. Tumor microenvironment-responsive histidine modified-hyaluronic acid-based MnO<sub>2</sub> as in vivo MRI contrast agent. *Int J Biol Macromol.* 2023;226:121–131. doi:10.1016/j.ijbiomac.2022.12.033
135. Khodayari H, Heydarinasab A, Moniri E, Miralinaghi M. Synthesis and characterization of magnetic nanoparticles-grafted-hyaluronic acid/ $\beta$ -cyclodextrin as a novel pH-sensitive nanocarrier for targeted delivery of doxorubicin. *Inorg Chem Commun.* 2023;148:110366. doi:10.1016/j.inoche.2022.110366
136. Mansoorianfar M, Hussain Z, Simchi A, Cao Y, Ullah I, Ullah S. Target-responsive DNA aptamer-conjugated superparamagnetic Ag/CuS nanoparticles as near-infrared light-triggered theranostics and dual-modal imaging. *Appl Mater Today.* 2023;34:101913. doi:10.1016/j.apmt.2023.101913
137. Zhang Y, Yu Y, Kang K, et al. Nano-magnetic aptamer sensor incorporating AND logic recognition-launched hybridization chain reaction for organ origin identification of circulating tumor cells. *Nano Today.* 2023;49:101817. doi:10.1016/j.nantod.2023.101817
138. Lodhi MS, Khalid F, Khan MT, et al. A Novel Method of Magnetic Nanoparticles Functionalized with Anti-Folate Receptor Antibody and Methotrexate for Antibody Mediated Targeted Drug Delivery. *Molecules.* 2022;27(1):261.
139. Taheri-Ledari R, Zolfaghari E, Zarei-Shokat S, Kashtiaray A, Maleki A. A magnetic antibody-conjugated nano-system for selective delivery of Ca(OH)<sub>2</sub> and taxotere in ovarian cancer cells. *Commun Biol.* 2022;5(1):995. doi:10.1038/s42003-022-03966-w
140. Pramanik A, Patibandla S, Gao Y, et al. Bio-Conjugated Magnetic-Fluorescence Nanoarchitectures for the Capture and Identification of Lung-Tumor-Derived Programmed Cell Death Lighand 1-Positive Exosomes. *ACS Omega.* 2022;7(18):16035–16042. doi:10.1021/acsomega.2c01210
141. Hasani M, Jafari S, Akbari Javar H, Abdollahi H, Rashidzadeh H. Cell-Penetrating Peptidic GRP78 Ligand-Conjugated Iron Oxide Magnetic Nanoparticles for Tumor-Targeted Doxorubicin Delivery and Imaging. *ACS Appl Bio Mater.* 2023;6(3):1019–1031. doi:10.1021/acsabm.2c00897
142. Thirumurugan S, Dash P, Liu X, et al. Angiopep-2-decorated titanium–alloy core–shell magnetic nanoparticles for nanotheranostics and medical imaging. *Nanoscale.* 2022;14(39):14789–14800. doi:10.1039/D2NR03683E
143. Horák D, Turnovcová K, Plichta Z, et al. RGDS- and doxorubicin-modified poly[N-(2-hydroxypropyl)methacrylamide]-coated  $\gamma$ -Fe<sub>2</sub>O<sub>3</sub> nanoparticles for treatment of glioblastoma. *Colloid Polym Sci.* 2022;300(4):267–277. doi:10.1007/s00396-021-04895-6
144. Pucci C, Degl’Innocenti A, Belenli Gümüş M, Ciofani G. Superparamagnetic iron oxide nanoparticles for magnetic hyperthermia: recent advancements, molecular effects, and future directions in the omics era. *Biomater Sci.* 2022;10(9):2103–2121. doi:10.1039/D1BM01963E
145. Zhi D, Yang T, Yang J, Fu S, Zhang S. Targeting strategies for superparamagnetic iron oxide nanoparticles in cancer therapy. *Acta Biomater.* 2020;102:13–34. doi:10.1016/j.actbio.2019.11.027
146. Rao Y-F, Chen W, Liang X-G, et al. Epirubicin-Loaded Superparamagnetic Iron-Oxide Nanoparticles for Transdermal Delivery: cancer Therapy by Circumventing the Skin Barrier. *Small.* 2015;11(2):239–247. doi:10.1002/smll.201400775
147. Schleich N, Po C, Jacobs D, et al. Comparison of active, passive and magnetic targeting to tumors of multifunctional paclitaxel/SPIO-loaded nanoparticles for tumor imaging and therapy. *J Control Release.* 2014;194:82–91. doi:10.1016/j.jconrel.2014.07.059

148. Ma K, Xu S, Tao T, et al. Magnetosome-inspired synthesis of soft ferrimagnetic nanoparticles for magnetic tumor targeting. *Proc Natl Acad Sci*. 2022;119(45):e2211228119. doi:10.1073/pnas.2211228119
149. Rosenblum D, Joshi N, Tao W, Karp JM, Peer D. Progress and challenges towards targeted delivery of cancer therapeutics. *Nat Commun*. 2018;9(1):1410. doi:10.1038/s41467-018-03705-y
150. Li Z, Yin S, Cheng L, Yang K, Li Y, Liu Z. Magnetic Targeting Enhanced Theranostic Strategy Based on Multimodal Imaging for Selective Ablation of Cancer. *Adv Funct Mater*. 2014;24(16):2312–2321. doi:10.1002/adfm.201303345
151. Muthana M, Kennerley AJ, Hughes R, et al. Directing cell therapy to anatomic target sites in vivo with magnetic resonance targeting. *Nat Commun*. 2015;6(1):8009. doi:10.1038/ncomms9009
152. Y-J L, Hsu H-L, Lan Y-H, Chen J-P. Thermosensitive Cationic Magnetic Liposomes for Thermoresponsive Delivery of CPT-11 and SLP2 shRNA in Glioblastoma Treatment. *Pharmaceutics*. 2023;15(4):1169. doi:10.3390/pharmaceutics15041169
153. Meng Y, Hynynen K, Lipsman N. Applications of focused ultrasound in the brain: from thermoablation to drug delivery. *Nat Rev Neurol*. 2021;17(1):7–22. doi:10.1038/s41582-020-00418-z
154. Schoen S, Kilinc MS, Lee H, et al. Towards controlled drug delivery in brain tumors with microbubble-enhanced focused ultrasound. *Adv Drug Deliv Rev*. 2022;180:114043. doi:10.1016/j.addr.2021.114043
155. Chen K-T, Wei K-C, Liu H-L. Theranostic Strategy of Focused Ultrasound Induced Blood-Brain Barrier Opening for CNS Disease Treatment. *Front Pharmacol*. 2019;10. doi:10.3389/fphar.2019.00086
156. Kobus T, Zervantonakis IK, Zhang Y, McDannold NJ. Growth inhibition in a brain metastasis model by antibody delivery using focused ultrasound-mediated blood-brain barrier disruption. *J Control Release*. 2016;238:281–288. doi:10.1016/j.jconrel.2016.08.001
157. Liu H-L, Hsu P-H, Lin C-Y, et al. Focused Ultrasound Enhances Central Nervous System Delivery of Bevacizumab for Malignant Glioma Treatment. *Radiology*. 2016;281(1):99–108. doi:10.1148/radiol.2016152444
158. Giammalva GR, Gagliardo C, Marrone S, et al. Focused Ultrasound in Neuroscience. State of the Art and Future Perspectives. *Brain Sci*. 2021;11(1):84. doi:10.3390/brainsci11010084
159. Grasso G, Torregrossa F, Noto M, et al. MR-guided focused ultrasound-induced blood-brain barrier opening for brain metastasis: a review. *Neurosurg Focus*. 2023;55(2):E11. doi:10.3171/2023.5.FOCUS23227
160. Papachristodoulou A, Signorell RD, Werner B, et al. Chemotherapy sensitization of glioblastoma by focused ultrasound-mediated delivery of therapeutic liposomes. *J Control Release*. 2019;295:130–139. doi:10.1016/j.jconrel.2018.12.009
161. Hou J, Zhou J, Chang M, et al. LIFU-responsive nanomedicine enables acoustic droplet vaporization-induced apoptosis of macrophages for stabilizing vulnerable atherosclerotic plaques. *Bioact Mater*. 2022;16:120–133. doi:10.1016/j.bioactmat.2022.02.022
162. Novoselova MV, Shramova EI, Sergeeva OV, et al. Polymer/magnetite carriers functionalized by HER2-DARPin: avoiding lysosomes during internalization and controlled toxicity of doxorubicin by focused ultrasound induced release. *Nanomed Nanotechnol Biol Med*. 2023;47:102612. doi:10.1016/j.nano.2022.102612
163. Bunevicius A, McDannold NJ, Golby AJ. Focused Ultrasound Strategies for Brain Tumor Therapy. *Oper Neurosurg*. 2020;19(1):9–18. doi:10.1093/ons/oz374
164. Kircher MF, Willmann JK. Molecular Body Imaging: MR Imaging, CT, and US. Part I. Principles. *Radiology*. 2012;263(3):633–643. doi:10.1148/radiol.12102394
165. Schenkman L. Second Thoughts About CT Imaging. *Science*. 2011;331(6020):1002–1004. doi:10.1126/science.331.6020.1002
166. Ahmed HU, Kirkham A, Arya M, et al. Is it time to consider a role for MRI before prostate biopsy?. *Nat Rev Clin Oncol*. 2009;6(4):197–206. doi:10.1038/nrclinonc.2009.18
167. Kim BH, Lee N, Kim H, et al. Large-Scale Synthesis of Uniform and Extremely Small-Sized Iron Oxide Nanoparticles for High-Resolution T1 Magnetic Resonance Imaging Contrast Agents. *J Am Chem Soc*. 2011;133(32):12624–12631. doi:10.1021/ja203340u
168. Lee SH, Kim BH, Na HB, Hyeon T. Paramagnetic inorganic nanoparticles as T1 MRI contrast agents. *WIREs Nanomed Nanobiotechnol*. 2014;6(2):196–209. doi:10.1002/wnan.1243
169. Tromsdorf UI, Bruns OT, Salmen SC, Beisiegel U, Weller H. A Highly Effective, Nontoxic T1 MR Contrast Agent Based on Ultrasmall PEGylated Iron Oxide Nanoparticles. *Nano Lett*. 2009;9(12):4434–4440. doi:10.1021/nl902715v
170. Tong S, Hou S, Zheng Z, Zhou J, Bao G. Coating Optimization of Superparamagnetic Iron Oxide Nanoparticles for High T2 Relaxivity. *Nano Lett*. 2010;10(11):4607–4613. doi:10.1021/nl102623x
171. Kuczyński EA, Vermeulen PB, Pezzella F, Kerbel RS, Reynolds AR. Vessel co-option in cancer. *Nat Rev Clin Oncol*. 2019;16(8):469–493. doi:10.1038/s41571-019-0181-9
172. Li Y, Qu X, Cao B, et al. Selectively Suppressing Tumor Angiogenesis for Targeted Breast Cancer Therapy by Genetically Engineered Phage. *Adv Mater*. 2020;32(29):e2001260. doi:10.1002/adma.202001260
173. Adisheshaiah PP, Hall JB, McNeil SE. Nanomaterial standards for efficacy and toxicity assessment. *WIREs Nanomed Nanobiotechnol*. 2010;2(1):99–112. doi:10.1002/wnan.66
174. Reichel D, Sagong B, Teh J, et al. Near Infrared Fluorescent NanoplatforM for Targeted Intraoperative Resection and Chemotherapeutic Treatment of Glioblastoma. *ACS Nano*. 2020;14(7):8392–8408. doi:10.1021/acsnano.0c02509
175. Hadjipanayis CG, Machaidze R, Kaluzova M, et al. EGFRvIII Antibody-Conjugated Iron Oxide Nanoparticles for Magnetic Resonance Imaging-Guided Convection-Enhanced Delivery and Targeted Therapy of Glioblastoma. *Cancer Res*. 2010;70(15):6303–6312. doi:10.1158/0008-5472.Can-10-1022
176. Kaluzova M, Bouras A, Machaidze R, Hadjipanayis CG. Targeted therapy of glioblastoma stem-like cells and tumor non-stem cells using cetuximab-conjugated iron-oxide nanoparticles. *Oncotarget*. 2015;6(11):34. doi:10.18632/oncotarget.3554
177. Shevtsov MA, Nikolaev BP, Yakovleva LY, et al. Superparamagnetic iron oxide nanoparticles conjugated with epidermal growth factor (SPION-EGF) for targeting brain tumors. *Int J Nanomed*. 2014;9:273–287. doi:10.2147/IJN.S55118
178. Arias-Ramos N, Ibarra LE, Serrano-Torres M, et al. Iron Oxide Incorporated Conjugated Polymer Nanoparticles for Simultaneous Use in Magnetic Resonance and Fluorescent Imaging of Brain Tumors. *Pharmaceutics*. 2021;13(8). doi:10.3390/pharmaceutics13081258
179. Shevtsov MA, Nikolaev BP, Ryzhov VA, et al. Brain tumor magnetic targeting and biodistribution of superparamagnetic iron oxide nanoparticles linked with 70-kDa heat shock protein study by nonlinear longitudinal response. *J Magn Magn Mater*. 2015;388:123–134. doi:10.1016/j.jmmm.2015.04.030

180. Tomitaka A, Arami H, Gandhi S, Krishnan KM. Lactoferrin conjugated iron oxide nanoparticles for targeting brain glioma cells in magnetic particle imaging. *Nanoscale*. 2015;7(40):16890–16898. doi:10.1039/C5NR02831K
181. Luo B, Wang S, Rao R, et al. Conjugation Magnetic PAEEP-PLLA Nanoparticles with Lactoferrin as a Specific Targeting MRI Contrast Agent for Detection of Brain Glioma in Rats. *Nanoscale Res Lett*. 2016;11(1):227. doi:10.1186/s11671-016-1421-x
182. Zhang F, Huang X, Zhu L, et al. Noninvasive monitoring of orthotopic glioblastoma therapy response using RGD-conjugated iron oxide nanoparticles. *Biomaterials*. 2012;33(21):5414–5422. doi:10.1016/j.biomaterials.2012.04.032
183. Nair BG, Nagaoka Y, Morimoto H, Yoshida Y, Maekawa T, Sakthi Kumar D. Aptamer conjugated magnetic nanoparticles as nanosurgeons. *Nanotechnology*. 2010;21(45):455102. doi:10.1088/0957-4484/21/45/455102
184. Wang S, Shen H, Mao Q, et al. Macrophage-Mediated Porous Magnetic Nanoparticles for Multimodal Imaging and Postoperative Photothermal Therapy of Gliomas. *ACS Appl Mater Interfaces*. 2021;13(48):56825–56837. doi:10.1021/acsami.1c12406
185. Xie M, Li Y, Xu Y, et al. Brain Tumor Imaging and Delivery of Sub-5 nm Magnetic Iron Oxide Nanoparticles in an Orthotopic Murine Model of Glioblastoma. *ACS Appl Nano Mater*. 2022;5(7):9706–9718. doi:10.1021/acsnm.2c01930
186. Jordan A, Scholz R, Wust P, Fähling H, Roland F. Magnetic fluid hyperthermia (MFH): cancer treatment with AC magnetic field induced excitation of biocompatible superparamagnetic nanoparticles. *J Magn Magn Mater*. 1999;201(1):413–419. doi:10.1016/S0304-8853(99)00088-8
187. Hilger I, Hiergeist R, Hergt R, Winnefeld K, Schubert H, Kaiser WA. Thermal Ablation of Tumors Using Magnetic Nanoparticles: an In Vivo Feasibility Study. *Invest Radiol*. 2002;37(10):580–586. doi:10.1097/00004424-200210000-00008
188. Salunkhe AB, Khot VM, Pawar SH. Magnetic Hyperthermia with Magnetic Nanoparticles: a Status Review. *Curr Top Med Chem*. 2014;14(5):572–594. doi:10.2174/1568026614666140118203550
189. Maier-Hauff K, Ulrich F, Nestler D, et al. Efficacy and safety of intratumoral thermotherapy using magnetic iron-oxide nanoparticles combined with external beam radiotherapy on patients with recurrent glioblastoma multiforme. *J Neurooncol*. 2011;103(2):317–324. doi:10.1007/s11060-010-0389-0
190. Peña Pino I, Ma J, Hori YS, et al. Stereotactic Laser Ablation (SLA) followed by consolidation stereotactic radiosurgery (cSRS) as treatment for brain metastasis that recurred locally after initial radiosurgery (BMRS): a multi-institutional experience. *J Neurooncol*. 2022;156(2):295–306. doi:10.1007/s11060-021-03893-6
191. Tasci TO, Vargel I, Arat A, Guzel E, Korkusuz P, Atalar E. Focused RF hyperthermia using magnetic fluids. *Med Phys*. 2009;36(5):1906–1912. doi:10.1118/1.3106343
192. Chang M, Hou Z, Wang M, et al. Single-Atom Pd Nanozyme for Ferroptosis-Boosted Mild-Temperature Photothermal Therapy. *Angew Chem Int Ed*. 2021;60(23):12971–12979. doi:10.1002/anie.202101924
193. Sun Z, Deng G, Peng X, et al. Intelligent photothermal dendritic cells restart the cancer immunity cycle through enhanced immunogenic cell death. *Biomaterials*. 2021;279:121228. doi:10.1016/j.biomaterials.2021.121228
194. Harmon BV, Corder AM, Collins RJ, et al. Cell Death Induced in a Murine Mastocytoma by 42–47°C Heating in Vitro: evidence that the Form of Death Changes from Apoptosis to Necrosis Above a Critical Heat Load. *Int J Radiat Biol*. 1990;58(5):845–858. doi:10.1080/09553009014552221
195. Tomitaka A, Kobayashi H, Yamada T, Jeun M, Bae S, Takemura Y. Magnetization and self-heating temperature of NiFe<sub>2</sub>O<sub>4</sub> nanoparticles measured by applying ac magnetic field. *J Phys Conf Ser*. 2010;200(12):122010. doi:10.1088/1742-6596/200/12/122010
196. Thiesen B, Jordan A. Clinical applications of magnetic nanoparticles for hyperthermia. *Int J Hyperth*. 2008;24(6):467–474. doi:10.1080/02656730802104757
197. Li GC, Mivechi NF, Weitzel G. Heat shock proteins, thermotolerance, and their relevance to clinical hyperthermia. *Int J Hyperth*. 1995;11(4):459–488. doi:10.3109/02656739509022483
198. Chiosis G, Digwal CS, Trepel JB, Neckers L. Structural and functional complexity of HSP90 in cellular homeostasis and disease. *Nat Rev Mol Cell Biol*. 2023. doi:10.1038/s41580-023-00640-9
199. Hoter A, El-Sabban ME, Naim HY. The HSP90 Family: structure, Regulation, Function, and Implications in Health and Disease. *Int J Mol Sci*. 2018;19(9):2560. doi:10.3390/ijms19092560
200. Lim S, Cho HY, Kim DG, et al. Targeting the interaction of AIMP2-DX2 with HSP70 suppresses cancer development. *Nat Chem Biol*. 2020;16(1):31–41. doi:10.1038/s41589-019-0415-2
201. Sha G, Jiang Z, Zhang W, Jiang C, Wang D, Tang D. The multifunction of HSP70 in cancer: guardian or traitor to the survival of tumor cells and the next potential therapeutic target. *Int Immunopharmacol*. 2023;122:110492. doi:10.1016/j.intimp.2023.110492
202. Huang L, Mivechi NF, Moskophidis D. Insights into Regulation and Function of the Major Stress-Induced hsp70 Molecular Chaperone In Vivo: analysis of Mice with Targeted Gene Disruption of the hsp70.1 or hsp70.3 Gene. *Mol Cell Biol*. 2001;21(24):8575–8591. doi:10.1128/MCB.21.24.8575-8591.2001
203. Qiu J, Li Z, An K, Niu L, Huang H, Xu F. Thermo-Chemical Resistance to Combination Therapy of Glioma Depends on Cellular Energy Level. *ACS Appl Mater Interfaces*. 2023;15(33):39053–39063. doi:10.1021/acsami.3c05683
204. Beliakoff J, Bagatell R, Paine-Murrieta G, Taylor CW, Lykkesfeldt AE, Whitesell L. Hormone-Refractory Breast Cancer Remains Sensitive to the Antitumor Activity of Heat Shock Protein 90 Inhibitors. *Clin Cancer Res*. 2003;9(13):4961–4971.
205. Fliss AE, Benzeno S, Rao J, Caplan AJ. Control of estrogen receptor ligand binding by Hsp90. *J Steroid Biochem Mol Biol*. 2000;72(5):223–230. doi:10.1016/S0960-0760(00)00037-6
206. Münster PN, Marchion DC, Basso AD, Rosen N. Degradation of HER2 by Ansamycins Induces Growth Arrest and Apoptosis in Cells with HER2 Overexpression via a HER3, Phosphatidylinositol 3'-Kinase-AKT-dependent Pathway. *Cancer Res*. 2002;62(11):3132–3137.
207. Fortugno P, Beltrami E, Plescia J, et al. Regulation of survivin function by Hsp90. *Proc Natl Acad Sci*. 2003;100(24):13791–13796. doi:10.1073/pnas.2434345100
208. Wu H, Liu L, Ma M, Zhang Y. Modulation of blood-brain tumor barrier for delivery of magnetic hyperthermia to brain cancer. *J Control Release*. 2023;355:248–258. doi:10.1016/j.jconrel.2023.01.072
209. Curley CT, Sheybani ND, Bullock TN, Price RJ. Focused Ultrasound Immunotherapy for Central Nervous System Pathologies: challenges and Opportunities. *Theranostics*. 2017;7(15):3608–3623. doi:10.7150/thno.21225
210. Johansen PM, Hansen PY, Mohamed AA, Girshfeld SJ, Feldmann M, Lucke-Wold B. Focused ultrasound for treatment of peripheral brain tumors. *Explor Drug Sci*. 2023;1(2):107–125. doi:10.37349/eds.2023.00009

211. Bunevicius A, McDannold NJ, Golby AJ. Focused Ultrasound Strategies for Brain Tumor Therapy. *Oper Neurosurg*. 2020;19(1):9–18. doi:10.1093/ons/ozz374
212. Meng Y, Pople CB, Kalia SK, et al. Cost-effectiveness analysis of MR-guided focused ultrasound thalamotomy for tremor-dominant Parkinson's disease. *J Neurosurg*. 2020;135(1):273–278. doi:10.3171/2020.5.JNS20692
213. Jung HH, Kim SJ, Roh D, et al. Bilateral thermal capsulotomy with MR-guided focused ultrasound for patients with treatment-refractory obsessive-compulsive disorder: a proof-of-concept study. *Mol Psychiatry*. 2015;20(10):1205–1211. doi:10.1038/mp.2014.154
214. Clary A, Tyler WJ, Wetmore DZ. Abstract #45: ultrasound neuromodulation for the treatment of peripheral nerve compression syndromes. *Brain Stimulation*. 2019;12(2):e16. doi:10.1016/j.brs.2018.12.052
215. Coluccia D, Fandino J, Schwyzer L, et al. First noninvasive thermal ablation of a brain tumor with MR-guided focused ultrasound. *J Ther Ultrasound*. 2014;2(1):17. doi:10.1186/2050-5736-2-17
216. Zhang X, Lu H, Tang N, et al. Low-Power Magnetic Resonance-Guided Focused Ultrasound Tumor Ablation upon Controlled Accumulation of Magnetic Nanoparticles by Cascade-Activated DNA Cross-Linkers. *ACS Appl Mater Interfaces*. 2022;14(28):31677–31688. doi:10.1021/acsami.2c07235

International Journal of Nanomedicine

Dovepress

## Publish your work in this journal

The International Journal of Nanomedicine is an international, peer-reviewed journal focusing on the application of nanotechnology in diagnostics, therapeutics, and drug delivery systems throughout the biomedical field. This journal is indexed on PubMed Central, MedLine, CAS, SciSearch®, Current Contents®/Clinical Medicine, Journal Citation Reports/Science Edition, EMBase, Scopus and the Elsevier Bibliographic databases. The manuscript management system is completely online and includes a very quick and fair peer-review system, which is all easy to use. Visit <http://www.dovepress.com/testimonials.php> to read real quotes from published authors.

Submit your manuscript here: <https://www.dovepress.com/international-journal-of-nanomedicine-journal>